Universität-Frauenklinik Tübingen

Charakterisierung zelltypspezifischer Effekte von Plasma-aktiviertem Medium (PAM) auf das Endometriumkarzinom anhand verschiedener 2D und 3D Zellkultursystemen.

Inaugural-Dissertation
zur Erlangung des Doktorgrades
der Medizin

der Medizinischen Fakultät
der Eberhard Karls Universität
zu Tübingen

vorgelegt von

Becker, Eva

2024

Dekan: Professor Dr. B. Pichler

1. Berichterstatter: Professor Dr. M. Weiss
2. Berichterstatter: Professor Dr. A. Nüssler

Tag der Disputation: 07.05.2024

Inhaltsverzeichnis

Abbildungs- und Tabellenverzeichnis

Abkürzungsverzeichnis

Endometrial cancer (EC)

Deficiency in mismatch repair (dMMR)

Microsatellite instability (MSI)

Overall survival (OS)

Human epithelial growth factor receptor 2 (HER2)

The Cancer Genome Atlas (TCGA)

polymerase epsilon DNA polymerase (POLE)

mismatch repair (MMR)

microsatellite instability-high (MSI-H)

selective estrogen receptor modulators (SERMs)

selective estrogen receptor degraders (SERDs)

Plasma-activated Medium (PAM)

Phosphate buffered saline (PBS)

Non-invasive physical plasma (NIPP)

Atmospheric Pressure Plasma Jet (APPJ)

reactive oxygen and nitrogen species (RONS)

Dielectric Barrier Discharge (DBD)

Endometrial cancer (EC)

Estrogen receptor (ER)

Progesterone receptors (PR)

basement membrane extract (BME)

Propidiumiodid (PI)

Room temperature (RT)

DNA double-strand (dsDNA)

1 Introduction

1.1. Endometrial Cancer

Endometrial cancer is a malignant neoplasia of the uterus. It concerns the epithelial parts of the endometrium.

1.1.1. Epidemiology

Endometrial cancer (EC) is the sixth most common malignancy in women worldwide and the most common gynaecological malignancy in the developed world. The incidence is estimated at 15–20 per 100,000 women per year.(1) In 2018 more than 380,000 new cases were registered as well as 89,000 fatal cases. The highest incidences are found in Europe and North America. While the average age of women to be sickened with EC in Germany is 69 years it is important to note that up to 14% of cases occur in premenopausal women. (2) This occurrence can largely be attributed to elevated body mass index (BMI). 80% of EC are diagnosed in FIGO-Stadium I. The mortality rate in Germany is 30% and clearly regressive over the past years. The overall 5-year survival rate is around 80%. (1, 3-6) Moreover, patients with tumors localized in the uterus exhibit a promising 5-year survival rate of ≥ 95%. However, this rate decreases significantly when the disease has spread beyond the uterus, with rates of 69% in patients with regional metastasis and 17% in those with distant metastatic disease. (7)

1.1.2. Aetiology

While the majority of endometrial cancers are sporadic, a subset of cases is hereditary and attributed to germline mutations, primarily occurring in mismatch repair (MMR) genes (11). It is assumed that the transition from normal endometrial tissue to cancer tissue involves a stepwise accumulation of alterations in genes favoring cell proliferation, the inhibition of apoptosis and angiogenesis.

There are several factors, which lead to an increased risk of developing EC.

Factors that pose higher risks for endometrial cancer include an increased estrogen exposure such as increased endogenous estrogen production and exogenous estrogen administration. High body mass index (BMI), metabolic syndrome, late-onset type II

diabetes, and hypertension are associated with elevated estrogen levels, particularly in postmenopausal women where ovarian hormonal output decreases [15]. Women with a history of menstrual irregularities, early menarche (early onset of menstruation), late menopause, and low parity (fewer pregnancies) have a higher risk of endometrial cancer (15). Medications such as tamoxifen, tibolone, or estrogens without gestagen protection, can increase the risk of endometrial cancer. (15) Approximately 10% of endometrial cancer cases are considered familial, with some associated with hereditary non-polyposis colorectal cancer (HNPCC), also known as Lynch syndrome. (2, 8, 11, 16-19)

On the other hand, certain factors are considered protective against endometrial cancer include multiple pregnancies, healthy and active lifestyle such as regular physical activity and a balanced diet, the use of oral contraceptives containing gestagens and hormone-releasing intrauterine devices (IUDs) can contribute to a lower risk of endometrial cancer. (1) Interestingly, also smoking after the onset of menopause has been associated with a reduced risk of endometrial cancer, particularly among estrogen users (70% risk reduction) and non-estrogen users (50% risk reduction). (20)

1.1.3. Symptoms and diagnostics

Abnormal uterine bleedings like menorrhagia or metrorrhagia, irregular cycles or postmenopausal bleedings are the most common symptoms presenting with EC. 90% of women diagnosed with EC showed at least one of these symptoms. (8) If a postmenopausal bleeding occurs, a hysteroscopy in combination with fractioned abrasion should be initiated. Taking a biopsy of the endometrial tissue is possible as well. (9) A transvaginal sonography should be performed to evaluate the infiltration of myometrium and cervix. To detect the intraabdominal tumor spreading, a staging is done during surgery. Metastases are relatively rare. However, if there is a suspicion for a metastasis, a thorax x-ray can be done to search for lung metastasis, sonography for abdominal metastasis as well as CT and MRT.

1.1.4. Histological and molecular Endometrial Cancer Classification

Endometrial cancer can be classified in two types based on clinic-pathological and molecular characteristics: the more common, estrogen associated type I and the non-estrogen dependent type II. Type 1 EC is characterized by specific features including endometrioid histology, presence of endometrial hyperplasia, expression of estrogen receptors (ER) and progesterone receptors (PR), and often exhibits deficiency in mismatch repair (dMMR) or microsatellite instability (MSI). Patients with type 1 EC typically have certain demographic and clinical characteristics such as being younger in age, having obesity or overweight status, and being nulliparous. This type of EC is generally classified as low grade and remains localized to the uterus, resulting in a favorable prognosis with treatment. (10) The 5-year overall survival (OS) rate for type 1 EC is approximately 86%. Type 2 EC is characterized by distinct features including nonendometrioid histology, commonly presenting as serous or clear cell carcinoma, or high-grade adenocarcinoma. Unlike type 1 EC, type 2 EC is not dependent on estrogen for its growth and proliferation due to the lack of estrogen receptor (ER) and progesterone receptor (PR) expression. Type 2 EC may exhibit human epidermal growth factor receptor 2 (HER2) positivity. Patients diagnosed with type 2 EC are typically older, often women of color, smokers, and less likely to be obese or nulliparous. Type 2 EC is associated with a poorer prognosis compared to type 1 EC, with a 5-year overall survival (OS) rate of approximately 59%. (10) Despite providing valuable prognostic information and guiding to treatment decisions the current classification of endometrial cancer based on histology offers limitations, such as the significant interobserver variability in histologic classification and the discrepancy between histologic subtypes and the specific tumor grade. (10)

These are tumors variants concerning morphology or histopathology which are characterized by aggressive behaviour and poor prognosis (1).

Immunohistochemical markers, such as p53, PTEN, ER, PR, and others, have been useful in differentiating between endometrial cancer subtypes. P53 is a tumor suppressor gene located on chromosome 17 and codes for a nuclear protein. It plays an important role in inhibiting the cell cycle of cells with damaged DNA. Mutations of p53 are reported to

be seen in 71% - 85% of EC Type II, but less common in Type I, where it ranges between 16% and 40%. The mutant p53 protein is non-functional but resists degradation and accumulates thereby acting as a dominant negative inhibitor of the wild-type p53. Looking at the histological grading, it can be detected that grade 1 and 2 tumors are positive for p53 mutations at much lower rates than high grade (grade 3) tumors. This suggests that p53 occurs as a late molecular event in Type I tumors. (1, 11-13) Estrogen (ER) and progesterone (PR) receptors are members of the nuclear receptor superfamily. The uterus is considered to be ERalpha dominant. (14, 15)

In 2013, The Cancer Genome Atlas (TCGA) Research Network conducted an extensive genomic analysis of 373 endometrial carcinomas, encompassing various molecular techniques such as whole exome sequencing, transcriptome sequencing, copy number analysis, protein array analysis, microsatellite stability testing, and methylation profiling. The results revealed four specific categories of endometrial carcinomas with unique clinical, pathological, and molecular characteristics: POLE (ultra-mutated) (7%), microsatellite instability (MSI)/hypermutated (28%), copy number low/microsatellite stable (39%), and serous-like/copy number high (26%). (16) These TCGA subgroups align with and further divide the histologic subgroups of endometrial carcinomas.

The POLE ultra-mutated subgroup is characterized by exceptionally high somatic mutation rate of the polymerase epsilon DNA polymerase (POLE). These cancers exhibit an excellent prognosis with no recurrences, despite a significant portion displaying high-grade histology, morphological heterogeneity, severe nuclear atypia, and TP53 mutations. (17, 18)

MSI hypermutation arises from deficiencies in the DNA mismatch repair (MMR) system. Common mutations in the MSI subgroup include ARID5B mutations, PTEN mutations, and mutations in the phosphatidylinositol-3-kinase family genes, including PIK3CA and PIK3R1 (16) enabling the development and use of targeted therapies.

Further distinct molecular subgroups include a copy number (CN) low subgroup and a CN high subgroup, based on copy number alterations. Generally, tumors in the CN high subgroup exhibit the least favorable prognosis among the four molecular subgroups. (19)

1.1.5. Therapeutic strategies after fertility completion

The individually tailored treatment of endometrial cancer includes surgical, systemic, and radiation therapy approaches, which are determined based on the molecular and stage-dependent individual risk profile.

Operative treatment strategies can be performed with curative or palliative intent, depending on the FIGO stage. Systemic therapies and radiation may be already indicated for intermediate and high-intermediate risk profiles to significantly reduce the risk of recurrence and metastasis.

The standard surgical treatment for endometrial cancer involves laparoscopic or open total abdominal hysterectomy, bilateral salpingo-oophorectomy, and staging lymphadenectomy or sentinel node identification. Unfortunately, this treatment approach results in the loss of fertility.

The systemic front-line treatment for women with advanced endometrial cancer (EC) typically involves platinum-based chemotherapy in combination with a taxane, according to established guidelines. (20) The addition of trastuzumab (Herceptin) depends on the HER2 status of the patient. Other possible treatment options include bevacizumab, doxorubicin, and various recommended agents as monotherapy based on individual patient factors, however, multiagent regimens are generally favored for most women. Hormone treatment is an alternative front-line option for certain women with low-grade endometrioid tumors, smaller tumor volume, or slow tumor growth. (20) Prognostic factors for response to hormonal therapy include well-differentiated, ER/PR-positive tumors, a long disease-free interval in recurrent disease, and the location or extent of metastases.

It is important to note that these front-line treatment options can be associated with significant toxicity, and consideration of patient preferences and quality of life should be part of shared decision-making. (21) The treatment options for subsequent lines of therapy in patients with recurrent or metastatic endometrial cancer (EC) are challenging, and there is no defined standard of care for second-line treatment. When patients experience disease progression or develop chemoresistance, alternative approaches are needed. One potential option is immunotherapy, specifically immune

checkpoint inhibitors. Pembrolizumab, an anti-PD-1 monoclonal antibody, has been approved by the FDA for the treatment of advanced EC with specific biomarker criteria. It is indicated for patients with unresectable or metastatic EC that is microsatellite instability-high (MSI-H) or mismatch repair deficient (dMMR). (10) Another approach is targeted therapy based on specific molecular alterations identified in individual tumors. The PI3K/AKT/mTOR pathway is frequently dysregulated in EC, and inhibitors targeting this pathway, such as everolimus, temsirolimus, and other PI3K inhibitors, have shown promise in clinical trials.

1.1.6. Fertility-sparing treatment

With the rise of global endometrial cancer incidence and the increasing age of childbearing, more women with desire for child bearing are expected to be diagnosed with endometrial cancer (8,9). Preserving fertility gains importance and addresses the development of new non-invasive treatment strategies. Currently available pharmacological methods for fertility preservation include oral progestins, levonorgestrel-releasing intrauterine devices, gonadotropin-releasing hormone agonists, aromatase inhibitors, metformin as well as selective estrogen receptor modulators (SERMs) and selective estrogen receptor degraders (SERDs). (22-24)

Hysteroscopic resection can be attempted for localized endometrial hyperplastic or malignant lesions. The hysteroscopic resection process typically involves resection of the lesion, resection of adjacent endometrium, and resection of underlying myometrium, followed by treatment with progestins or placement of a levonorgestrel-releasing intrauterine device. (25) The evidence from these procedures has been incorporated into the 2021 ESGO guidelines. (20)

However, both local and systemic hormonal procedures, even when aimed at fertility preservation, significantly reduce the chances of spontaneous conception and uncomplicated pregnancy and childbirth. Therefore, there is an urgent need for innovative, non-invasive and hormone-independent local treatment strategies.

1.2. Non-invasive physical plasma (NIPP) therapy

Non-invasive physical plasma (NIPP) has gained a fast-growing attention over the last few years due to its wide range of applications and promising opportunities. It could be a new alternative treatment method for various disease patterns, especially in cancer therapy. NIPP indicates promising anti-neoplastic and anti-proliferative effects on several tumor entities like melanoma, glioma and several gynecological tumors e.g., breast cancer, ovarian cancer as well as cervical cancer. NIPP treatment leads to sufficient inhibition of cancer cell growth without severe side effects like tissue swelling, inflammation or pain. (26-29) NIPP is already used in several fields in medicine including root canal treatment, blood coagulation, cancer and skin treatments. Due to its impressive antiviral and antibacterial effects plasma is also used for the sterilization of surfaces as well as for wound healing. (30, 31)

The basic principle of plasma therapy consists of an application of electric discharge on a biological surface. The electrical discharge is generally obtained by applying high voltage to an active electrode with the help of gas. A variety of gases, like helium, argon, neon, nitrogen, oxygen or even their mixtures can be used. (26, 32)

1.2.1. Physico-chemical NIPP characteristics

NIPP can be described as a highly energetic gas and refers to the fourth state of matter. NIPP, which is used in medicine, reaches temperatures which are not significantly higher than body temperature, between 25 and 45°C, so it doesn't result in thermal damages. (32)

The composition of radical and ionic particles as well as free electrons leads to a further transfer of energy to the surrounding particles in the air, resulting in the formation of reactive oxygen and nitrogen species (RONS). These are the main biomedically active species in NIPP which also occur naturally in physiologically active tissues. RONS and various other biologically reactive species can induce physical, chemical as well as biological reactions on a cellular level. (33) As endogenous substances, RONS are thus also signaling molecules with specific cell biological effects that can be used for specific therapies.

However, the influence on biological tissue or cells only occurs as long as NIPP is applied; Caused by short-living reactive species such as hydroxyl radicals, which remain stable for only nanoseconds, or singlet oxygen, which survives for up to a few microseconds. (31)

There are several different methods and appliances to produce NIPP such as Atmospheric Pressure Plasma Jet (APPJ), Plasma Needle, Plasma Pencil or Dielectric Barrier Discharge (DBD).(27, 32, 34) The DBD plasma device consists of two electrodes, a high voltage and a grounded electrode. (32) These are flat metal electrodes covered with dielectric material. (32) Plasma is created through an ionized gas which moves between the two electrodes. (32) A DBD plasma device is used in the following experiments.

There are two different ways of how to apply plasma on the place of action: direct and indirect application. An example for a direct application is the APPJ, NIPP is applied directly on the tissue. To apply plasma indirectly, a fluid is activated with plasma before applying it on tissue, which is then called Plasma-activated Medium (PAM).

1.2.2. Plasma activated medium (PAM)

Treatment of liquid media with NIPP generates PAM.(29) PAM functions as a carrier of plasma-specific components and its biological effects and contains long-lived species from NIPP such as nitrite, nitrate and hydrogen peroxide. (35, 36)

PAM has several advantages compared to NIPP: PAM can be stored in a refrigerated state for 7 days without loss of efficacy. This allows PAM to be flexibly averted in situations where NIPP treatment is not possible, e.g. laparoscopic procedures. (37)

Under physiological conditions, mucous membranes are wetted with fluids. When applying NIPP on mucous membrane, they could be dried out. In contrast, PAM can maintain the physiologically moisturized conditions in large parts.

PAM allows homogeneous and simultaneous treatment of surfaces, which is a major advantage for intraoperative use. (38, 39)

1.2.3. NIPP biomedical mode of action

Primarily responsible for NIPP-triggered cell mechanisms and cell death are most likely reactive oxygen and nitrogen species (RONS). Other highly reactive components of NIPP include charged particles like nitrite, nitrate and peroxynitrit, free radicals like hydroxyl-radicals as well as ultraviolet and infrared radiation. (34)

NIPP demonstrated to induce apoptosis, necrosis, cell detachment and senescence by disruption the S phase of cell replication in tumor cells. This enables a potential use in oncology. (32)

At the same time, the effects of reactive species are influenced by antioxidant substances. This means that especially substances such as glutathione, N-acetylcysteine, catalase and superoxide dismutase must be considered when using plasma therapies. (40) Tumor cells have shown to be less endowed with antioxidant defense mechanisms. (41)

Compared tumor cells with nonmalignant cells, NIPP and PAM were found selectively towards malignant target cells in vitro and in vivo. The selective cytotoxicity of cancer cells over normal cells was already demonstrated in several studies. (42) Plasma seems to be targeting a general principle of tumor cells. (29) However, the underlying mechanism by which plasma induced cell death remains unknown. (27)

1.3. Organoid models

The main obstacles in understanding mechanisms in endometrial tissue is the lack of suitable models. Immortalized or carcinoma-derived endometrial cancer cell lines do not correctly mimic the situation in vivo. Adult endometrial cancer cell lines are proven to be difficult to maintain in long-term culture as the cultured cells quickly lose their phenotype and hormone responsiveness. (43) In general, traditional two dimensional cell cultures do not faithfully represent three dimensional organ biology and functioning. (44) For that reason, organoids have been developed throughout the last years to mimic a more realistic tool for studying the tissue's biology.

Organoids are self-forming 3D reconstructions of an organ's epithelium, typically developing under defined culture conditions. They reproduce many aspects of the

tissue's epithelium histology, functionality and (patho-)biology. (45-47) They are therefore superior to 2D cell cultures. Advantages to two-dimensional cell lines are the reliably recapitulate components of the tumor environment such as the structure and interaction of cancer cells with stroma and blood vessels.(48) Tissue for patient-derived organoids is obtained from consenting patients who underwent tumor resection. (49)
Organoids are seeded out in basement membrane extract (BME) matrigel. Matrigel-based organoid culture enables long-term expandability and infinite proliferation under physiological conditions.
Organoids are already established in gynecologic tumors like ovarian and endometrial cancer. The organoids containing cancer cells showed retaining aspects of the original tumors, including histological features, mutation profiles as well as intra-tumoral heterogeneity. They are illustrating an intra- and interpatient heterogeneity. Therefore they serve as a promising resource for preclinical studies. (50)

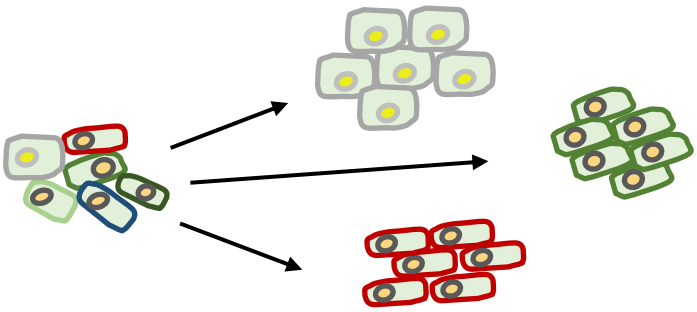

Figure 1: Schematic of organoid growth. Tumor tissue is being split up into single cells, consecutively forming organoids clones out of one primary cell.

Patient-derived cancer organoids have developed an increasing relevance over the last years, particularly in terms of drug discovery. Studies showed that patient-derived organoids can be used for drug-screening assays and capturing of tumor responses. (49) Furthermore, organoids can also be xenografted, which enables in vivo drug-sensitivity assays. (49)

However, establishing new cell lines also faces some difficulties. It can be a challenging and time-consuming process that involves contamination and low success rates. Additionally, the process is very expensive due to resources of their maintenance.

Taken together, organoids demonstrate a high potential for research and personalized medicine. It is a novel model that provides a tool for studying mechanisms underlying the biology as well as the pathology. (44)

1.4. Aim and objectives

Endometrial carcinoma is the fourth most common malignancy in women occurring predominantly in post-menopausal patients. Although the outcome is generally favorable, the prognosis of patients in advanced stages remains poor. The treatment involves an invasive surgery containing hysterectomy, adnexectomy and lymphonodectomy most of the times. Fertility preserving treatment strategies are currently lacking. Therefore, there is an increasing demand for new therapeutic options like plasma therapy.

The purpose of this study was:

- Basic establishment and characterization of PAM treatment of 2D and 3D cell culture systems by using established cell lines
- Establishment of a patient-derived 3D organoid culture
- Establishment and characterization of PAM treatment of 3D organoid models regarding treatment effectiveness of different tumor gradings
- Characterization of intracellular PAM mechanisms regarding cell viability, DNA double-strand breaks and oxidative stress.

2 Materials and Methods

2.1. Materials

2.1.1. Reagens

Experiment	Reagent	Stocks	Producer	Product No.
Cell culture (2D)	DMEM	500 mL	Thermo Fisher Scientific	41965-039
	Penicillin/ Streptomycin 1%	100 mL	Thermo Fisher Scientific	15140-122
	Dulbecco's Phosphate buffered Saline	500 mL	Thermo Fisher Scientific	10010023
	Fetal bovine serum	500 mL	Gibco	10270-106
	Trypsin EDTA 0,05%	100 mL	Thermo Fisher Scientific	25300-054
Cell culture (3D)	Cultrex reduced growth factor BME2	1 mL	Bio-Techne	3533-001-02
	recovery cell culture freezing medium	50 mL	Gibco	12648010
	TrypLE	100 mL	Gibco	12604013
(Tumor processing)	Collagenase (S)	100 mg	Sigma	C9407
	Collagenase Type II	1 g	Gibco	17101015
Medium				

	B27-AO supplement	10 mL	Thermo Fisher Scientific	10889038
	EGF	1 mg	Peprotech	AF-100-15
	FGF-10	50 µg	Peprotech	100-26
	GlutaMax	100 mL	Gibco	35050-038
	Heregulin-β-1	100 µg	Peprotech	100-03
	Nicotinamide	100 g	Sigma	NO636
	Penicillin - Streptomycin	100 mL	Gibco	15140-122
	SB202190	5 mg	Sigma	S7067
	Y-27632	50 mg	Hölzel	TMO-T1725-50 mg
Immune fluorescence	Albumin from bovine serum	100 g	Fluka BioChemika	05488
	DAPI 1000 X	1 mg/mL	Invitrogen	D1306
	ProLong™ Diamond Antifade Mountant with DAPI	2 mL	Invitrogen	P36962
	Triton X-100	12 mL	SEKISUI	R14694
	Tween® 20	250 g	Roth	9127.1
Fixation of cells/organoids	Dispase II	1 g	Sigma	D4693
	Ethanol (absolute)	2.5 L	Merck KGaA	1.00983.2511
	Ethanol 99% denatured	5 L	Pharmacy	C1016

	Formaldehyde solution about 37%	1 L	Merck KGaA	1.04003.1000
	Sodium azide	100 g	Merck	1.06688.0100
	Xylol	2.5 L	PanReac AppliChem	131769.1612
Paraffin embedding	Histogel	10 mL	Fisher Scientific	12006679
	Paraplast Plus	1 kg	McCormick Scientific	39502004
Antigen Retrieval (HIER)	Ethylenediaminetetraacetic acid	250 g	AppliChem	A5097,0250
	Sodium hydroxide solution	1 L	Merck KGaA	1.09137.1000
	Tri-Sodium-Citrate	1 kg	AppliChem	A3901,1000
	Trizma® base	1 kg	Sigma	T1503-1KG
Crystal Violet Staining	Hexamethylpararosanilinchlorid	100 G	Sigma	C0775-100G
3D Cell Viability Assay	CellTiterGlo	10mL	Promega	526140
Plasma device			DBD Liquid Treatment System	FB: 8.35.6 Version: 01
Argon 4.8 Spectro	99,998 Vol% Argon	50L	Westphalen	2760050288 7945-62
Live/dead assay	Hoechst 33342 Lösung	20 mM	ThermoFisher Scientific	62249

	Calcein, AM	1 mL	ThermoFisher Scientific	C3099
	Propiodiumiodid	100 mg	ThermoFisher Scientific	P1304MP

2.1.2. Cell lines

Cell line	Lot. No	Medium
HEC-1A	SIDM00595	DMEM +1% P/S + 1% GlutaMax +10% FBS
ISHIKAWA	99040201	DMEM +1% P/S + 1% GlutaMax +10% FBS

2.1.3. Patient-specific cell culture

	Characteristics	Medium
Endo-ctrl	Patient age 45; healthy endometrial tissue	BC-E
Endo-G1	Patient age 63; endometrioid adenocarcinoma; Grading G1	BC-E
Endo-G2	Patient age 71; endometrioid adenocarcinoma; Grading G2	BC-E
Endo-G3	Patient age 66; endometrioid adenocarcinoma; Grading G3	BC-E

2.1.4. Equipment

Device	Type	Company
Centrifuge	Multifuge 3 S-R	Thermo Scientific Heraeus, Waltham, USA
Centrifuge	Biofuge pico	Thermo Scientific Heraeus, Waltham, USA
Centrifuge	Rotina 380	Hettich, Tuttlingen, Deutschland

Automated Cell Counter	TC20tm	Bio rad , Hercules, USA
EVOS microscope	M7000	Invitrogen, Waltham, USA
Epson Perfection Scanner	V800	Epson, Suwa, Japan
Incubator	9040-0012 CB 150	Binder, Tuttlingen, Deutschland
Light microscope	CK30	Olympus, Tokyo, Japan
Microtome	HM 335 S	Fisher Scientific, Waltham, USA
Varioscan LUX multimode microplate reader	VL0000D0	Thermo Fisher Scientific, Waltham, USA
Tissue culture plate	48-well plate	Falcon, Corning, USA
Tissue culture plate	Nunclon Delta Surface 96-well plate flat white bottom	Fisher Scientific, Waltham, USA
Tissue culture plate	96-well plate flat bottom	Falcon, Corning, USA
Tissue culture plate	96-well plate u-shaped bottom	Falcon, Corning, USA
Glass slides	30000030	R. Langenbrinck GmbH, Emmendingen, Deutschland
Coverslips	631-0169	VWR, Radnor, USA
T25 cell culture flask	690175	Greiner Bio One, Frickenhausen, Deutschland
T75 cell culture flask	658175	Greiner Bio One, Frickenhausen, Deutschland
Petri dish	5cm	Falcon, Corning, USA
Eppendorf cups 0,5 mL	S72699	Sarstedt, Nümbrecht, Deutschland

Eppendorf cups 1,5 mL	616201	Greiner Bio One, Frickenhausen, Deutschland
Eppendorf cups 2,0 mL	303174	Greiner Bio One, Frickenhausen, Deutschland
Falcon 15 mL	188271-N	Greiner Bio-One, Frickenhausen, Deutschland
Falcon 50 mL	227261	Greiner Bio-One, Frickenhausen, Deutschland
Cryovial	122263	Greiner Bio-One, Frickenhausen, Deutschland
Shaker for plates	Titramax 1000 544-12200-00 6 plates	Heidolph Instruments, Schwabach, Deutschland
Waterbath	Typ: 1003; no.:11233302 K 37°C	GFL, Burgwedel, Deutschland
Fluorescence Microscope	Axio observer	Zeiss, Jena, Deutschland
Plasma device	DBD Liquid Treatment System	Plasma DBD GmbH, Göttingen, Germany

2.1.5. Kits

Kit name	Type	Source
GSH/GSSG Assay	Oxidative stress assay	Promega, Madison, USA

2.1.6. Media compositions for 2D cell lines

The medium consists of DMEM (with 1% P/S and 1% GlutaMax) and 10% FBS.

2.1.7. Media compositions for organoids

The culture media for the organoids was established at the Department of Women's Health, University Hospital Tuebingen, Germany. The media was adapted for the performed experiments with assistance from Dr. André Koch.

Breast cancer media (BC-E)

Main medium component was DMEM^{+++} (with P/S and GlutaMax) which was used to fill up to corresponding volume.

Reagent	Final concentration
DMEM	
B27 - AO (50x)	1x
Nicotinamide (1 M)	10 mM
HGF	1.25 µM
RepSox	100 µg/mL
Heregulin-β-1 (75 µg/mL)	37.54 µg/µL
Insulin Sigma I0516	100 µM
EGF (10 µg/mL)	5 µg/µL
SB431542 (5 mM)	0.5 µM
Y27632 (100 mM)	5 µM

- DMEM $^{+++}$: DMEM with 1% Penicillin -Streptomycin and 1% GlutaMax

2.1.8. Antigen retrieval buffer

- Tris-EDTA (pH 9) with 0.05% Tween: 1L
    - 1.21 g Tris Base and 0.37 g EDTA
    - Add H_2O to 1L
    - Adjust to pH 9 with NaOH
    - Add 2,5 mL 20% Tween

2.1.9. Antibody list

Primary antibodies

Name	Target	Species	Dilution (FFPE slides)	Company	Ordering No.	pH / Buffer
Ki67	Ki67/Mib1	Rabbit	1:500	Abcam	16667	pH 9
p53 (DO-7)	p53	Mouse	1:50	DAKO	M700129-2	pH 9
PAX 8	PAX8	Rabbit	1:1000	Proteintech	10336-1-AP	pH 9
yH2AX	Histone H2AX-Ser139	Mouse	1:500	Upstate	05-636	pH9
ER alpha (SP1)	ERα	Rabbit	1:50	Abcam	Ab16660	pH9
Progesterone receptor concentrate	PR	Mouse	1:50	DAKO	M356929-2	pH9

Cytokeratin 7 – Clone OV-TL 12/30	CK7	Mouse	1:200	DAKO	M7018	pH9
Keratin 8/18	CK8/18	Mouse	1:250	Thermo Fisher Scientific	MS-743-S	pH9

Secondary antibodies

Name	Color	Species	Dilution	Company	Ordering No.
M488-2	green	Mouse	1:400	Invitrogen	A11029
R594-2	red	Rabbit	1:400	Invitrogen	A11012

2.2. Methods

2.2.1. 2D cell culture of cell lines HEC-1A and ISHIKAWA

Frozen cell lines were thawed in the water bath at 37°C, then added to 10 mL prewarmed DMEM P/S into a 15mL falcon. The flacon was centrifuged with 1500 rpm, for 10 min at room temperature. After the supernatant was removed, the cell pellet was resuspended in DMEM-FCS. Cell suspension was transferred to a T25 cell culture flask. Medium changes had to be done approximately every three to four days, depending on the growth of the cells.

2.2.2. 2D cell culture splitting

Splitting of 2D cells had to be done as soon as the cells in the cell culture flask were confluent. Medium was removed and cells were washed with PBS 0.05% once before 2 ml of Trypsin-EDTA were added to the cell culture flask, then incubated for 3 min at

37°C. After the 3 minutes incubation a detachment of the cells from the flask was seen under the microscope. If cells weren't completely detached, tapping against the flask could help the detachment. To stop the reaction of Trypsin-EDTA, DMEM-FCS had to be added to the flask, approximately double of the amount than Tryspin-EDTA. Resuspension of the cell suspension dissolved cell clumps. Parts of the cell suspension is mixed with DMEM-FCS and transferred into the cell culture flask according to required splitting ratio.

2.2.3. Tumor processing of endometrial cancer

Endometrial cancer tissue was obtained from patients after surgical removal at the Department of Women's Health, University Hospital Tübingen, Germany and processed into organoids. The scientific use of human tissue samples was approved by the institutional review board of the medical faculty of the University Hospital Tübingen (ethical vote: 495_2018BO02). Written informed consent was obtained from all patients. Tissue samples were transported in DMEM supplemented with 1% penicillin/streptomycin. To confirm the malign nature and to determine further pathological characteristics of the primary tissue, pathological review of the specimen was performed by a gynaecological pathologist at the pathology department of the university hospital in Tübingen.

The tumor sample was measured and photographed and divided into different parts based on the texture of the sample. The next step was chopping the sample into small pieces with a scalpel to an average size of 1-3 mm. 2mL reaction tubes were filled with the tumor sample and Collagenase (1:2), Advanced DMEM +++ (1:2) and ROCK-Inhibitor Y27632 (1:1000). This had to be incubated on the shaker with 1000 rpm at 37°C between 0.5-2h, depending on tumor texture. The content of the reaction tube was completely transferred to a 15 mL tube, filled up to 8 mL with PBS and resuspended. Cell strainer with 40 µm and 100 µm size were placed on top of a 50 mL tube and moistened with 2-3 mL PBS. The resuspended cell suspension was now filtered through the 100 µm and 40 µm cell strainer and washed with PBS. The cell suspension was centrifuged with 1500

rpm for 10 min at room temperature (RT), then the supernatant was removed, and the cell pellet was stored on ice.

The cell pellet was resuspended in small amount of Advanced DMEM +++. Parts were used for an organoid culture setup; parts were frozen with freezing medium in a freezing vial at -80°C.

2.2.4. Organoid culture set up

Organoid cultures can be set up directly after tissue processing which is explained in 2.2.3. Another possibility is setting up the cultures from frozen tissue samples.

Frozen samples had to be thawed in a water bath at 37°C and transferred into a falcon with prewarmed DMEM P/S. Then centrifuged with 1500 rpm for 10 min at RT. The supernatant has to be removed and the cell pellet was resuspended in Advanced DMEM $^{+++}$. The cell pellet with Advanced DMEM $^{+++}$ was mixed with Matrigel in 1:1.5 ratio and then plated out in a 48-well plate with a 20 µL drop size. The plate had to be placed upside down in an incubator with 37°C for approximately 30 min allowing the Matrigel to polymerize. 270 µL of BC-E medium was carefully added to each well after 30 minutes and PBS was filled into the empty wells around for moistening.

2.2.5. Passaging and freezing of organoids

The protocol applies for all endometrial organoid cultures. The BC-E medium was carefully removed from the wells and collected in a 15 mL falcon. 1 mL of ice-cold PBS/Y was used to scratch the Matrigel domes briefly and then resuspend the domes completely in the PBS/Y. The Matrigel containing the organoids was transferred into the falcon. All the wells had to be rinsed again with ice-cold PBS/Y and were transferred into the falcon to make sure to catch all the organoids in the well. The falcon was then centrifuged with 1500 rpm for 5 minutes. The supernatant was removed. The Matrigel with the organoids was visible as a cloudy pellet at the bottom of the falcon. Following, 1 mL of TrypLE was carefully added and resuspended in the Matrigel and organoids. The falcon had to incubate in a 37°C waterbath for 5-10 minutes, depending on the density of the organoids. After the incubation, the solution had the be pipetted up and down

several times for mechanical disruption of the organoids. Following, the falcon was filled up to 10 mL with ice-cold PBS/Y and centrifuged at 1500 rpm for 5 minutes or until a cell pellet could be seen. The supernatant was removed and organoids could be seeded out like described in 2.2.4.

If not all the organoids are needed for the setup of the new passage of organoid culture, parts were be frozen like described in 2.2.3.

2.2.6. Preparation of Plasma-activated Medium (PAM)

The Plasma device 'DBD Liquid Treatment System' was used for the production of PAM. The appliances to adjust the settings for the PAM production were based on the right side of the device: Feasible adjustments were time in minutes and seconds, the frequency and amplitude of the plasma as well as the gas flow of the argon gas. On the left side of the device was the reaction chamber, where the PAM was produced.

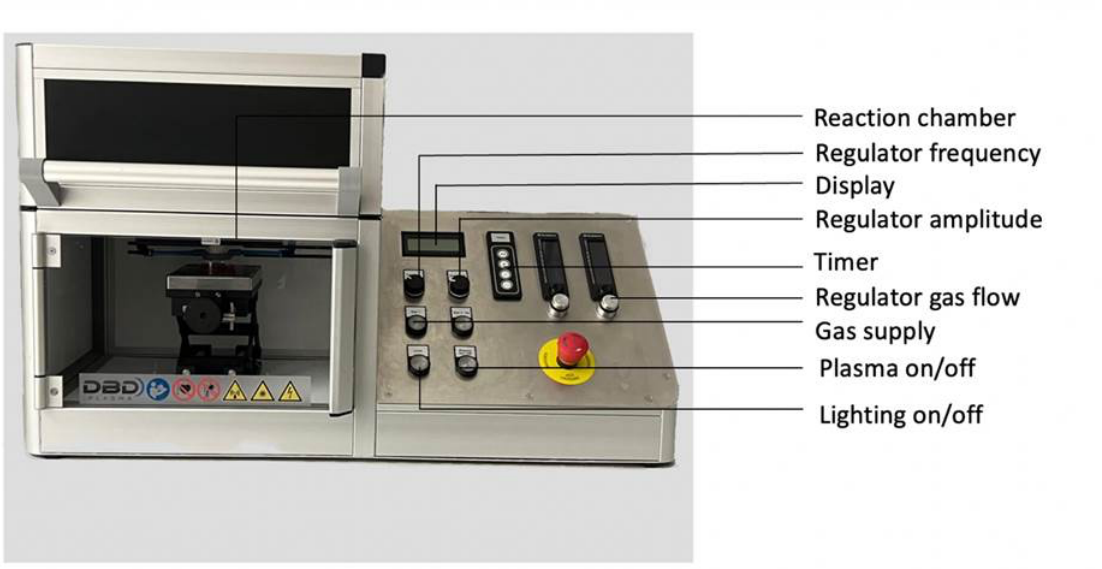

Figure 2: Plasma device 'DBD Liquid Treatment System'.

A petri dish filled with medium, DMEM in this case, is placed on the height adjustable table and directly under the white electrode. Argon gas flows through the blue tubes. Plasma flows through the electrode and together with the argon gas, air and medium it results in PAM.

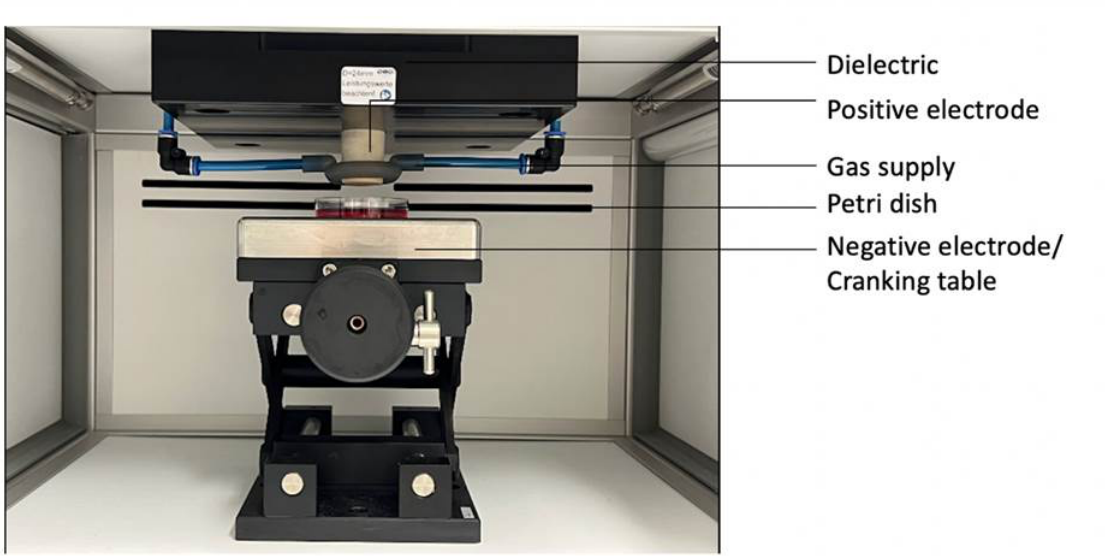

Figure 3: Reaction chamber of Plasma Device for production of PAM.

PAM had to be freshly produced for each experiment and put onto the cells immediately. The Plasma device which was used for the following experiments was the DBD Liquid Treatment System. Exactly 7 mL of DMEM were filled into a petri dish for the activation. The distance between the plasma source and the surface of the DMEM was fixed at 5mm. The same operating conditions had to be applied every time to make the produced PAM comparable: argon gas flow at 15.0 L/min, frequency of 5935 Hz and 40% amplitude. The operating conditions were recommended by the producer of the plasma device. The duration of the activation is adaptable. For the 2D cell lines an activation time of 2 min and 3 min was compared. For the organoids an activation time of 3 min was established.

2.2.7. Microscopic documentation with EVOS microscope of organoid culture

Pictures of the organoids in the 48-well plate were taken after seeding them out and before slitting the organoids. In between these times, pictures had to be taken every 3-4 days.

Pictures were taken with the Software M7000 (Fischer Scientific, Waltham, USA). General settings were 80% of the wells with 4x magnification in transillumination with Invitrogen EVOS microscope.

2.2.8. Immunofluorescence pictures

Immunofluorescence pictures were taken > 24h after staining. Pictures were taken with the Invitrogen EVOS microscope Software M7000 from Fischer Scientific in 10x and 20x magnification in DAPI (wavelength 358 nm), GFP (wavelength 475 nm) or TxRed (wavelength 605 nm) channels. Light and exposure varied among every picture, the value for gain constantly remained at 1.

2.2.9. Crystal Violet Staining

The staining is colorimetric and based on the attachment of the cells to the culture plate. Since adherent cells detach from the culture plate during cell death, the assay can be used as an indirect quantification of cell death. Crystal Violet is a triarylmethane which binds to proteins and DNA. The staining stains nuclei in a deep purple color.

As soon as the cells in the control well were confluent, the staining could be performed. Medium, in this case DMEM-FCS, had to be removed and the cells were fixed with 50 µL per well of 100% methanol for 10 minutes. Dead cells detached and were washed away during the shake off of the methanol. 0.5% Crystal Violet solution was added to cover the bottom of the wells and incubated for 3-4 hours at RT. After incubation the crystal violet was removed and the wells were washed in water multiple times until dye stopped coming off. All water residues had to be shaken off and dried at RT by turning the plates upside down. The plates had to be covered for protection from light. As soon as the plate was dry, it could be scanned by a flat-bed scanner and analyzed and evaluated with ImageJ.

2.2.10. CellTiterGlo Assay

The CellTiter Glo Luminescent Assay is an assay to determine the amount of viable cells in culture. It is based on the quantification of the ATP, an indicator of metabolically active cells.

The assay was performed 72 hours after PAM treatment of the cells. Medium had to be removed. 40µl advanced DMEM and 50µl CellTiterGlo Reagent were added to the wells. Then it had to be shaken at 900 rpm for 15 minutes until Matrigel is dissolved. The wells had to be covered at all times to be protected from light. The wells had to be resuspended and transferred from the U-shaped 96-well plate into a white bottom 96-well plate. Blanks were added to determine contamination. Then the luminescent signal was determined with the VarioLux Scanner.

2.2.11. Live/dead Assay

The live/dead Assay is a dichromatic assay for detection of viability of cells based on the integrity of the plasma membrane and esterase activity.

The Assay was performed 24h after PAM treatment of the organoids. The BC-E medium was removed and the wells were washed and incubated with PBS for 5 minutes. Hoechst and Calcein were diluted 1:500 in PBS+ and incubated at 37°C for 1h. Hoechst and Calcein were removed from the organoids after incubation. 5 µL Propidiumiodid (PI) in 100 µL PBS was incubated at 37°C for 5 minutes on the organoids. Then washed carefully with PBS multiple times and observed with the fluorescent microscope. Hoechst is a blue fluorescent, nuclear specific dye which can be used to stain live or fixed cells. Calcein is a cell-permeable dye for identification of cell viability. In viable cells Calcein is converted into green fluorescence through esterases. PI is a red fluorescent nuclear counterstaining which cannot permeate living cells. It is used to detect dead cells in a cell population. The stainings were evaluated and pictures were taken with the Fluorescence Microscope (Zeiss, Jena, Germany).

For reflector HE BFP a wavelength of 385 nm and a light source intensity of 45% was used. For the Green Fluorescent Prot Reflector a wavelength of 475 nm and light source

intensity of 25% and for Reflector DsRed a wavelength of 567 nm with a 100% light source intensity. Pictures were analyzed and edited with Zeiss Zen lite software.

2.2.12. GSH/ GSSG Assay

The GSH/GSSG-Glo Assay is a luminescence-based system that detects and quantifies glutathione in reduced (GSH) and oxidized (GSSG) forms. Both forms exist in healthy cells, but the majority in the reduced form GSH. A change in GSH/GSSG levels can be an indicator for toxicity like oxidative stress.

The Assay was performed 24h after PAM treatment of the cells. The medium had to be removed. A lyse of the cells with either Total or Oxidized Glutathione reagent was performed. Therefore either 50 µl/well for adherent cells or 25 µl/well for suspension cells was needed. The plate with the Reagent had to be shaken for 5 minutes. Then 50 µl/well of Luciferin Generation Reagent was added. After a 30-minute incubation time 100 µl/well of Luciferin Detection Reagent was added and equilibrated for 15 minutes. Then the luminescence was read by the VarioLux Scanner.

2.2.13. Paraformaldehyde-fixation of organoids

Medium was removed from each well and all wells were washed once with PBS. In order to dissolve the Matrigel, 250 µl/well of Dispase (1 mg/mL) was added to the wells before scraping of the Matrigel drops with the pipette tip. The plate was incubated at 37°C for 15 min in the incubator.

From this step on, all reaction tubes and pipette tips that were used have been coated with 1% BSA in PBS in advance. The suspension in the wells was resuspended with 1 mL 1% BSA/well and then transferred to a 15 mL tube with 2 mL 1% BSA inside. The wells were washed once with 1% BSA, then transferred to the 15 mL tube and centrifuged for 5 min with 1025 rpm. After the supernatant was removed, 1 mL 3.7% PFA was added to the pellet and resuspending. The sample was added to a 1.5 mL reaction tube.

After a 30 min incubation at room temperature, the sample was centrifuged with 2000 rpm for 3 min, the supernatant was removed and disposed into a waste tube. The pellet was washed once with PBS and centrifuged again with 2000 rpm for 3 min, the

supernatant was again disposed into a PFA waste tube. The pellet was resuspended with 250 µL 25% EtOH and incubated for 10 min. Then 300 µL of 70% EtOH was added to the suspension. After 10 min 600 µL 96% EtOH was added to the suspension and then the sample was stored at 4°C.

2.2.14. Cytospins of paraformaldehyde-fixed single cells

PFA-fixed cells were stored at 4°C until they were further used for cytospins. A filter paper was put on an object slide. 1µl of water with a 9 mm coverslip on top was placed in the hole of the filter paper and then into the holder. The cytospin funnel was placed on top and secured with a sealing ring by rotation of 90°. Less than 200 µl of cell suspension were added to the funnel. The device was placed into the centrifuge and centrifuged with 1600 rpm for 8 min. The supernatant was disposed into a PFA waste tube. The cytospin device was dissembled and the coverslips with cytospinned cells were either stored at 4°C with PBS or directly used for immune fluorescence staining.

2.2.15. Paraffin-embedding of paraformaldehyde-fixed organoids

Histogel and a 200 µl sample were placed in the heating block at 65°C. The supernatant was removed from the PFA-fixed organoids that were stored at 4°C. The upper part of the pipette tip was removed, placed on parafilm and then on put on a cold metal block. The prewarmed histogel was added to the organoid pellet and incubated for 30 seconds at 65°C before it was transferred to the mold for the organoid suspension with a 1% BSA coated pipette tip. The pellet was shortly frozen and then incubated for 5 min at -20°C. The frozen sample was transferred into an embedding cassette and incubated twice for 1h in 70% EtOH. After that, the sample was incubated twice for 1h in 96% EtOH and one time for 1h in EtOH and then overnight in 100% EtOH. The next day, the sample was placed for 2 x 1h in Xylol, followed by 3 x 45 min in paraffin. For each sample one embedding metal mold was prewarmed at 65°C, filled with paraffin and the organoid pellet was taken out of the embedding cassette and placed into the center of the mold. The embedding cassette was then put on top and additionally filled with paraffin. After

15 min at -20°C the embedding cassette with the organoid pellet was taken off of the embedding metal mold and stored at RT until they were cut at the microtome.

2.2.16. Dewaxing of paraffin-embedded organoid sections

Before dewaxing the slides, they were scratched at the back with a diamond pencil in order to know where organoids are located on the slide. For the dewaxing process, the slides were placed in Xylol for 3 x 10 min, in 100% EtOH for 2 x 3 min, in 96% EtOH for 2 x 3 min, in 75% EtOH for 1 x 3 min, in 75% EtOH for 1 x 5 min and washed in water for 5 min. Dewaxed slides were kept in PBS until further processing.

2.2.17. Antigen-retrieval of dewaxed paraffin-embedded organoid sections

Buffer was prepared according to 2.1.8. and stored at RT. A glass bucket was filled with 300 mL buffer and heated in the microwave at 800 W for approximately 2 min until the solution reached between 90°C and 100°C. Slides were placed in a metal rack into the bucket with prewarmed buffer and incubated for 10 min at 180 W. The temperature of the buffer should be kept between 90-100°C during the antigen retrieval. The bucket with the slides was placed into an ice bucket to cool down and the slides were later stored in PBS until further processing.

2.2.18. Immunofluorescence staining of cytospinned cells and paraffin-embedded organoid sections after antigen-retrieval

Paraffin-embedded organoid sections were air-dried and the organoids on slide were circled with ImmEdge fat pen to border the sample for the further steps. All incubations took place in the dark foiled box at RT. The solutions were added to the coverslips in circled spots until they were covered by a big dome-like drop. All coverslips and organoid sections were mounted with ‘Prol Diam DAPI’ that was prewarmed at 37°C.

The sample was washed once with PBS-T for 5 min and then permeabilized for 3 min with 0.2% Triton X in PBS. After 3 x 5 min washing with PBS-T the sample was blocked for 30 min with 4% BSA in PBS-T. The primary antibody was diluted in 4% BSA in PBS-T

according to table in 2.1.9. and incubated for 1h at RT. The sample was washed again 3 x 5 min with PBS-T before the secondary antibody was added. Secondary Antibody was diluted in 4% BSA in PBS-T according to table in 2.1.9. and incubated for 1h at RT. Next, 3 x 5 min washing step with PBS-T was followed by 5 min incubation with 1 x DAPI in PBS-T.

The coverslips were then dipped in 100% EtOH before air-drying and mounted with 2 µl mounting medium on slides.

The stained samples recovered overnight on a flat object slide in the dark at RT and then stored at 4°C.

2.2.19. Statistical analysis

Statistical data analysis was performed with the help of Microsoft Excel, Prism (GraphPad version 9.0, Graph Pad Software, San Diego, CA, USA), ImageJ (U.S. National Institutes of Health, Bethesda, Maryland, USA) and Zeiss Zen lite (Zen Lite I; Edition3.1). The data are expressed as mean $\pm$ standard deviation. A paired t-test was used to determine whether PAM treatment reduced cell viability significantly. $P < 0,05$ was considered to be statistically significant. Experiments were performed in at least three independent experimental approaches.

3 Results

Endometrial cancer is a common malignancy in postmenopausal women. However, also premenopausal patients suffer from endometrial cancers in 14 % of cases. Nowadays the standard treatment includes hysteroscopy and, depending on the tumor stage, adjuvant chemotherapy. PAM is a new, non-invasive treatment method which is currently tested on a variety of cancer types, such as endometrial cancer, to reduce treatment invasiveness and associated side effects. So far, PAM was only tested on 2D endometrial cancer cells, therefore this work – using 3D patient-derived endometrial cancer organoids - is an important contribution to the clinical translation of PAM-dependent treatment strategies. Using these patient-specific 3D in vitro models, cell type-specific, dose- and incubation time-dependent anti-proliferative efficacy of PAM was analyzed.

3.1. Effects of PAM concentration, PAM activation and incubation time on cellular viability of 2D cultured endometrial cancer cell lines

The effect of PAM on relative cell viability of 2D endometrial adenocarcinoma cell lines HEC-1A and ISHIKAWA was analyzed in this experiment. 5,000 cells per well were seeded out. PAM treatment was performed after 24h. Different PAM concentrations (2.5%, 5%, 10%, 12,5%, 20%, 25% and 50%), activation times (2 and 3 minutes), and incubation times (1h, 4h and 24h) were tested. Both cell lines were cultured in DMEM-FCS before and after PAM treatment. Relative cell viability was determined using a Crystal Violet assay after the control cells reached confluency. Representative pictures were taken from the Crystal Violet staining.

For both cell lines, HEC-1A and ISHIKAWA, a significantly reduced cell viability was observed. A significant reduction in cell viability was seen for concentrations of 20% PAM and higher for HEC-1A and concentrations 5% PAM and higher for ISHIKAWA.
HEC-1A showed an overall lower sensitivity to PAM compared to ISHIKAWA.

No difference of HEC-1A cell viability was observed when performing 4 and 24 h of PAM incubation, independent of whether cells were treated with 2 or 3 minutes activated PAM (Figure 4a and b). In contrast, when incubated 4 h, 3 min activated PAM resulted in significantly decreased cell viability (Fig. 4a, b; HEC-1A, 2 min PAM activation time, 1 h treatment time, 50% PAM dilution: 6.91-fold reduction, p=0.027; 3 min PAM activation time, 1 h treatment time, 20% PAM dilution: 5.94-fold reduction, p=0.036; 2 min activation time, 4 h treatment time, 20% PAM dilution: 26.88-fold reduction, p=0.031; 3 min PAM activation time, 4 h treatment time, 12.5% PAM dilution: 17.19-fold reduction, p=0.024; 2 min PAM activation time, 24 h treatment time, 20% PAM dilution: 30.14-fold reduction, p=0.041; 3 min PAM activation time, 24 h treatment time, 12.5% PAM dilution: 14.11-fold reduction, p=0.032).

Ishikawa showed an overall higher sensitivity to PAM compared with HEC-1A. When incubating PAM for 1h no significant difference of ISHIKAWA cell viability was observed among the investigated PAM concentrations, regardless of whether cells were treated with 2 or 3 minutes activated PAM. In contrast, when incubated 4 and 24 h 3 min activated PAM showed a significantly decreased cell viability at 5% PAM concentration (Fig. 4c, d; ISHIKAWA, 2 min PAM activation time, 1 h treatment time, 2.5% PAM dilution: 1.62-fold reduction, p=0.034; 3 min PAM activation time, 1 h treatment time, 2.5% PAM dilution: 2.08-fold reduction, p=0.035; 2 min PAM activation time, 4 h treatment time, 5% PAM dilution: 6.41-fold reduction, p=0.029; 3 min PAM activation time, 4 h treatment time, 2.5% PAM dilution: 3.-98fold reduction, p=0.012; 2 min PAM activation time, 24 h treatment time, 5% PAM dilution: 4.70-fold reduction, p=0.002; 3 min PAM activation time, 24 h treatment time, 2.5% PAM dilution: 2.94-fold reduction, p=0.025). Taken together, in addition to the PAM concentration used, both incubation time and duration of plasma activation play a critical role in cellular viability.

A 3 min PAM activation time and 24 h incubation time was used in the following experiments with 3D cells.

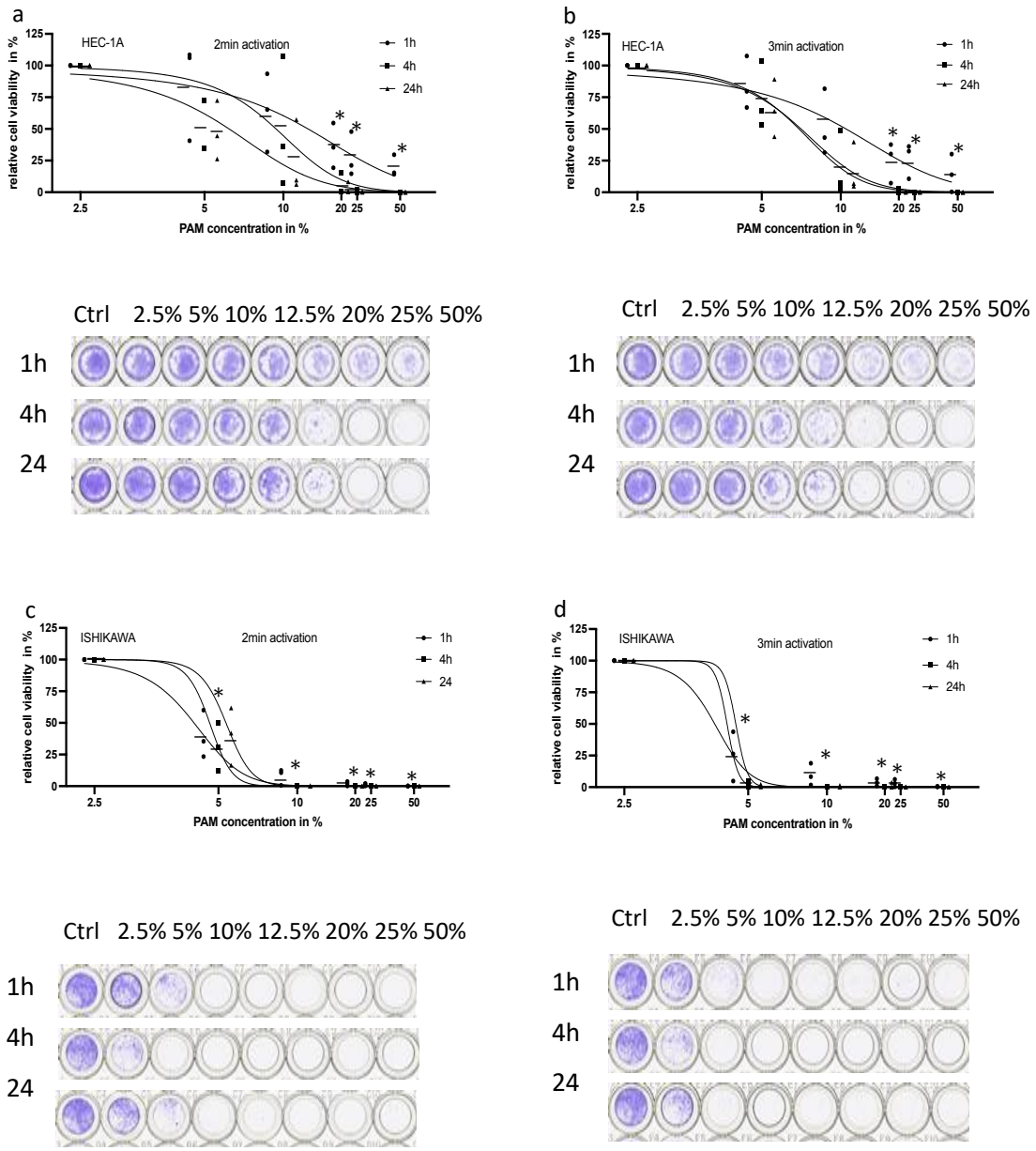

Figure 4: Dose-dependent cell viability after PAM treatment of 2D cultured endometrial cancer cell lines.

Relative cell viability (graph) and representative crystal violet staining (insert) of HEC-1A (a, b) and ISHIKAWA (c, d) after PAM treatment with indicated PAM concentrations, PAM activation times and PAM incubation times. Relative cell viability was determined when the control cells were confluent (72 h after PAM treatment). Data is presented as

mean ± SD from n=3 independent experiments. *p < 0.05, as determined by paired t-test.

3.2. PAM mediates dose-dependent and cell-line specific cytotoxicity in HEC-1A and ISHIKAWA organoids

To elucidate, whether PAM had an effect on 3D tissues, HEC-1A and ISHIKAWA were grown in BME matrix to generate organoids. Both cell lines were cultured in DMEM-FCS for 3 days before PAM treatment. PAM was activated for 3 minutes and different PAM concentrations (25%, 50%, 75% and 100%) were applied on the organoids. Moreover, to exclude significant influence of different customary cell culture media, DMEM-FCS and BC-E were used for 3D organoid culture. Following 24 h of PAM incubation time, the organoids were cultured with the different cell culture media for additional 48 h. Relative cell viability was analyzed by using the CellTiterGlo assay 72 h after PAM application. Representative pictures of the cells were taken before PAM application and before performance of the CellTiterGlo assay.

Corresponding to PAM effects in 2D cell culture, ISHIKAWA showed a higher sensitivity to PAM compared to HEC-1A (Figure 5) indicated by significantly reduced cell viability. ISHIKAWA cells significantly reduced cell viability at 25% PAM concentration (Fig. 5b, d; ISHIKAWA, 25% PAM dilution, DMEM-FCS: 45.28-fold reduction, p=0.010; BC-E: 12.15-fold reduction, p=0.006), whereas HEC-1A cells first showed a significant reduction in cell viability at 50% PAM concentration (Fig. 5a, c; HEC-1A, 50% PAM dilution, DMEM-FCS: 8.27-fold reduction, p=0.018 BC-E: 12.04-fold reduction, p=0.011).

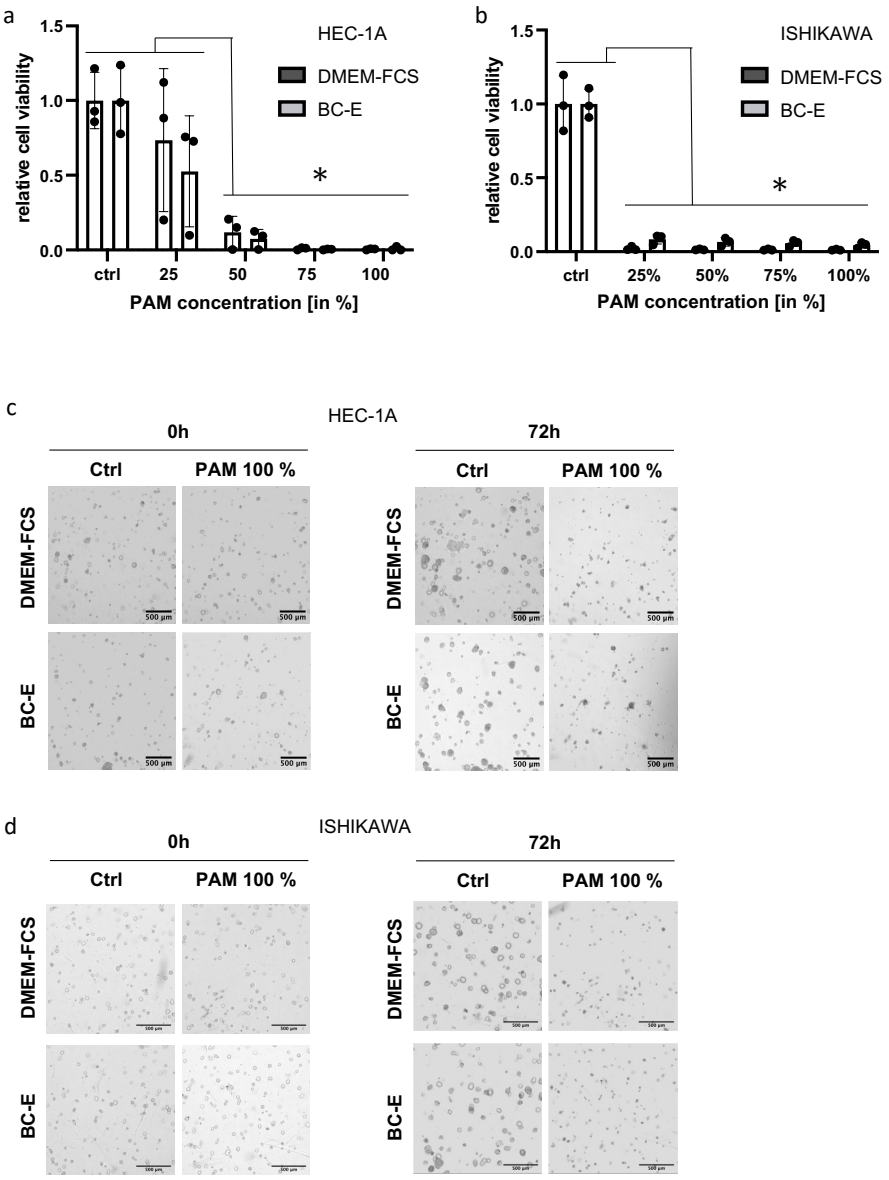

Figure 5: Dose-dependent PAM effect and comparison of DMEM-FCS vs. BC-E medium for endometrial cancer cells lines in 3D.

Relative cell viability (graph) and representative brightfield microscopy (insert) of HEC-1A (a,c) and ISHIKAWA (b,d) after PAM treatment with indicated PAM concentrations, 3 min PAM activation time and 24h PAM incubation time. Relative cell viability was determined 72h after PAM treatment through CellTiterGlo. Data is presented as mean ± SD from n=3 independent experiments. *$p < 0.05$, as determined by paired t-test.

Further fine-scaled experiments on HEC-1A organoids showed a significantly reduced relative cell viability at PAM concentrations of 35% and higher (Fig. 6, 35% PAM dilution: 35%: 12.64-fold reduction, p=0.03).

Representative brightfield microscopy 72 h after PAM treatment of HEC-1A (Figure 5c) and ISHIKAWA (Figure 5d) organoids indicate the cytotoxic cell effect. Organoids treated with 100% PAM concentration showed atrophied and dead cells, compared to the controls demonstrating continuous cell growth.

Taken together, dose-dependent PAM effects on reduction of cell viability of organoids from HEC-1A and ISHIKAWA without influence of different media, DMEM-FCS and BC-E, were identified in this experiment.

BC-E media was used in the following experiments with patient-derived organoids.

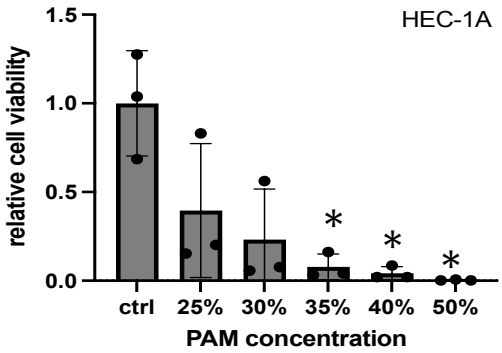

Figure 6: PAM treatment of endometrial cancer organoids with fine-scaled PAM concentrations.

Relative cell viability of HEC-1A after PAM treatment with indicated PAM concentrations. 3 min PAM activation time, 24h PAM treatment time. Relative cell viability was determined when the cells in the control wells were confluent (72 h after PAM treatment). Data is presented as mean ± SD from n=3 independent experiments. *$p < 0.05$, as determined by paired t-test.

3.3. DNA double-strand breaks are seen in HEC-1A cells after PAM treatment in 2D as well as in organoids

PAM is known for being a trigger of DNA double-strand (dsDNA) breaks. This can be detected by staining the PAM treated cells for yH2ax.

To elucidate whether PAM had the same effects on 2D cells as on organoids on a molecular level, an immunofluorescence staining for yH2ax was performed 12 and 24h after PAM treatment.

3000 cells/ well were seeded out and treated with PAM after being cultivated for 3 days. PAM was activated for 3 minutes. After a 12h and 24h incubation time, the cells were fixed in paraformaldehyde and embedded in paraffin, following an immunofluorescence staining for yH2ax. Pictures were taken 24h after staining (Figure 7).

No dsDNA breaks could be detected throughout the controls. Whereas after a 12h and 24h PAM incubation time, some dsDNA breaks were detected in 2D HEC-1A as well as in HEC-1A organoids. For 2D HEC-1A, more dsDNA breaks were detected after 24h PAM incubation time than after 12h incubation time. However, the opposite applied for the HEC-1A organoids: more dsDNA breaks were detected after 12h of PAM incubation.

In conclusion, PAM treatment induces dsDNA breaks in 2D endometrial adenocarcinoma cells as well as in organoids. No dsDNA breaks were detected in the controls.

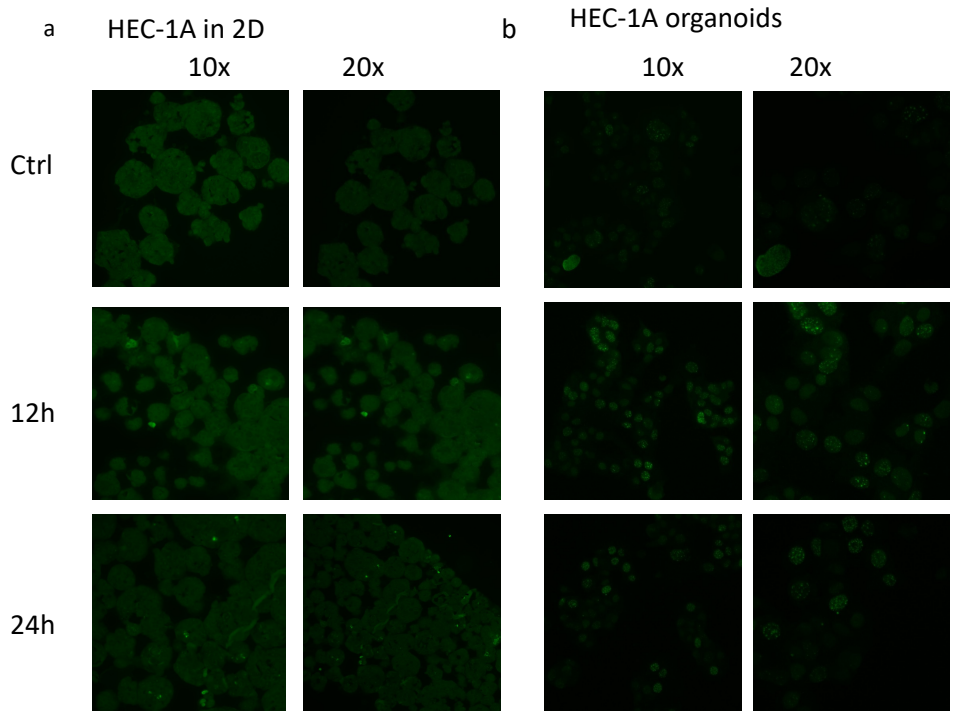

Figure 7: Comparison of dsDNA breaks in 2D HEC-1A cells vs. HEC-1A organoids through staining of yH2ax.

Representative immunofluorescence microscopy of 2D HEC-1A (a) and HEC-1A organoids (b). After PAM treatment with 50% PAM concentration, 3 min PAM activation time, and 12 or 24h PAM treatment time, yH2ax immunofluorescence staining was performed after indicated PAM treatment time to determine DNA double-strand breaks. Pictures of the cells were taken 24h after staining.

3.4. Patient-derived endometrial cancer organoids show comparable tumor characteristics compared to the original cancer tissue

In previously performed experiments, PAM effects on 2D cell lines and their respective organoid models were investigated. Different cell lines, HEC-1A and ISHIKAWA, showed cell line specific sensitivities to PAM in 2D and likewise in their organoid models.

Throughout the next experiments the influence of the tumor biology, especially tumor grading, will be investigated concerning the effectiveness of PAM on endometrial adenocarcinoma cells. Grading is classified into low-grade cancers (grade 1 and 2) and high-grade cancers (grade 3). In low-grade cancers, more than half of the cancer cells form glands, whereas in high-grade, most of the cancer cells are disorganized and less than half of the cancer tissue are forming glands. Grade 3 cancers tend to be more aggressive due to fast tumor growth and spread.

For that reason, patient-derived organoid systems obtained from patients with low- and high-grade endometrial adenocarcinomas were developed.

Endometrial cancer tissue was obtained from patients after surgical removal at the Department of Women's Health, University Hospital Tübingen, Germany and processed into organoids. The scientific use of human tissue samples was approved by the institutional review board of the medical faculty of the University Hospital Tübingen (ethical vote: 495_2018BO02). Written informed consent was obtained from all patients.

Four different patient-derived organoid cultures were used: Three samples of endometrial adenocarcinoma with different gradings G1-G3 and one sample of healthy endometrial tissue:

Healthy endometrial tissue was obtained from a 45-year-old patient. Healthy endometrial tissue was hyperplastic but with no evidence of malignancy. No further pathological assessment was performed.

G1 endometrial adenocarcinoma was extracted from the uterus of a 63-year-old patient. The tumor was highly differentiated and restricted to the cavum uteri and the inner half of the myometrium with maximal infiltration depth of 5mm/23mm.

G2 endometrial adenocarcinoma was obtained from a 71-year-old patient. The tumor was located in the corpus uteri and moderately differentiated with an infiltration depth of 8mm/22 mm.

G3 endometrial adenocarcinoma was obtained from a 66-year-old patient. The tumor was poorly differentiated and located in the corpus uteri with maximal infiltration depth of 14/20 mm.

Further information concerning immunohistochemical parameters can be found in table 1.

Table 1: Immuno-histological parameters and characteristics of patient-derived tumor tissue.

Name	Grading	P53	P16	ER	PR	Proliferation index	MSI status	L1-CAM
EndoCa-G1	G1	Wild type	heterogeny	positive, IRS9, 70%	positive IRS9, 80%	50%	stable	negative
EndoCa-G2	G2	Wild type	Unknown	positive, IRS 12, 100%	positive IRS12, 100%	low	Sporadically stable (under 1%)	unknown
EndoCA-G3	G3	Wild type	heterogeny	positive	positive	Unknown	loss of MLH1 and PSH2, expression of MSH2 and MSH6.	positive (30-40%)

Representative brightfield microscopy from organoids of EndoCA-G2 in passage 6 was taken after organoids were split and seeded out. The organoids grew rapidly and had to be split on day 7 (Figure 8).

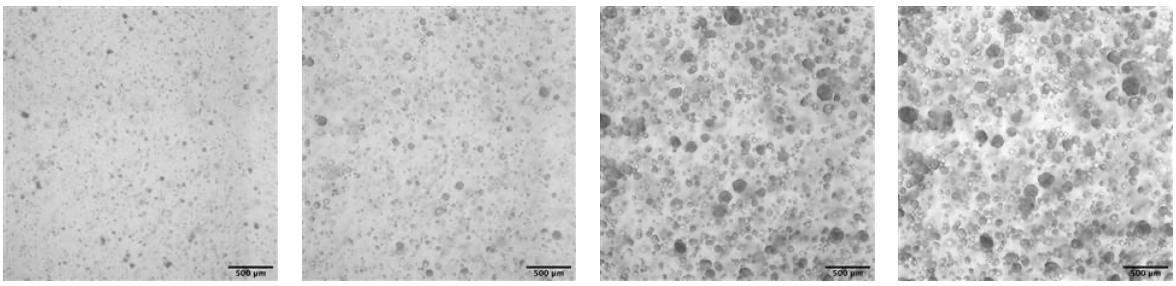

d 0 d 3 d 6 d 7

Figure 8: Representative brightfield microscopy of endometrial cancer organoids in P6 after seeding (day 0), day 3, day 6 and before splitting the organoids (day 7).

3.5. Patient-derived organoids express characteristic endometrial cancer markers

Representative for all patient-derived organoid models, characteristic tumor markers were compared between the original G2 tumor and the patient-derived EndoCA-G2 organoids. For this, an immunofluorescence staining of Paired-Box-Protein 8 (PAX8), tumor suppressor gene p53, estrogen receptor (ER) and progesterone receptor (PR), cytokeratin 7 (CK7) and cytokeratin 8/18 (CK8/18) was performed (Figure 9).

PAX8 is a member of the family of transcription factors. It plays an important role as an immunohistochemical marker in the diagnosis of gynecologic tract malignancies. It is expressed in epithelial neoplasms like endometrial carcinoma. PAX 8 was found in the immunohistochemical staining in patient-derived organoids.

p53 is a regulatory protein which is often mutated in human cancer. The overexpression of p53 in immunohistochemistry is a significant prognostic factor in endometrial cancer. Also p53 was expressed in patient-derived EndoCA-G2 organoids.

Cytokeratins are a large group of intermediate filament proteins which are preferentially expressed in epithelial tissue. They play an important role in determining epithelial structural integrity under stressful conditions. In addition to that, they have various other functions in proliferation, adherence, migration and molecular signaling. In most cases, CK7 as well as CK8/18 are stained positive in endometrial adenocarcinoma. This is also the case in the stainings performed on patient-derived EndoCA-G2.

Furthermore, ER and PR were identified on patient-derived EndoCA-G2. Both receptors are frequently present in endometrial cancer and are important biomarkers determining the prognosis. The pathology assessment of the patient-derived tumor showed a 99% presence of both receptors.

In summary, the performed stainings verified a high correlation between the patient-derived EndoCa-G2 organoids and the original tumor tissue.

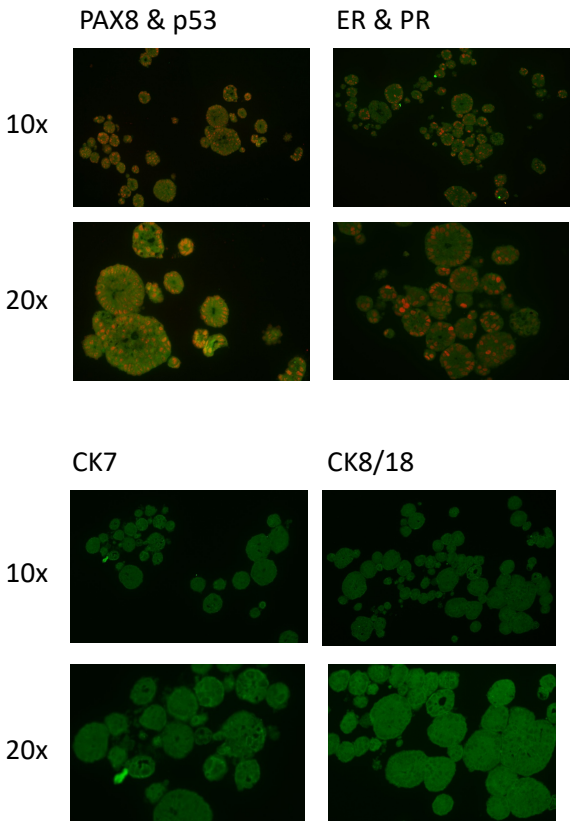

Figure 9: Representative tumor characterization of patient-derived EndoCA-G2 organoids.

Representative immunofluorescence microcopy of paraffin-embedded EndoCa-G2 organoids stained with different tumor specific markers to verify their endometrial cancer origin. PAX8 and ER are stained red. P53, PR, CK7 and CK8/18 are stained green. Images were taken in 10x and 20x magnification.

3.6. Patient-derived endometrial cancer organoids dose- and tumor-grading dependent cytotoxicity after PAM treatment

Patient-derived organoids were propagated in BME matrix with 1,000 cells/ well as described in 2.2.5. The organoids were grown for 3 days before PAM treatment. To elucidate the PAM effect on patient-derived endometrial cancer organoids, relative cell viability was determined through a CellTiterGlow Assay 72 hours after PAM treatment.

Significant reduction of relative cell viability was determined throughout all patient-derived endometrial cancer organoids: for Grading 1 (EndoCA-G1, Figure 10b) at PAM concentrations of 50% and higher (Fig. 10b; EndoCA-G1: 50% PAM dilution: 5.42-fold reduction, p=0.022; 75% PAM dilution: 12.69-fold reduction, p=0.018; 100% PAM dilution: 37.19-fold reduction, p=0.022); for Grading 2 (EndoCA-G2, Figure 10c) at PAM concentrations of 50% and higher (Fig. 10c; EndoCA-G2: 50% PAM dilution: 4.96-fold reduction, p=0.042; 75% PAM dilution: 126.65-fold reduction, p=0.020; 100% PAM dilution: 2627.45-fold reduction, p=0.019) and for Grading 3 (EndoCA-G3, Figure 10d) at PAM concentrations of 25% and higher (Fig. 3d; EndoCA-G3: 25% PAM dilution: 5.35-fold reduction, p=0.049; 50% PAM dilution: 17.11-fold reduction, p=0.039; 75% PAM dilution: 247.52-fold reduction, p=0.023; 100% PAM dilution: 10058.42-fold reduction, p=0.022).
Compared to the endometrial cancer organoids, PAM didn’t show any significant effects on patient-derived healthy endometrial tissue (Endo-ctrl, Figure 10a).
Taken together, organoids with the highest grading G3 (meaning the most undifferentiated cancer cells) showed a higher sensitivity towards PAM than organoids with lower gradings.

Representative brightfield microscopy was performed on patient-derived EndoCA-G2 organoids before PAM application and before performing the CellTiterGlo Assay (Figure 10e). The organoids in the control wells and 25% PAM concentration wells were continuously growing without any visible effects on morphology and proliferation. Organoids which were treated with 50% PAM concentrations showed significant impact

on cell growth. Small organoids even looked dead. Organoids treated with 75% PAM concentration were mostly dead, only large organoids were still alive. But even in large organoids the usually round looking organoid margin seemed to have an irregular structure. All organoids looked atrophied and dead in 100% PAM concentrations.

Resulting from the brightfield microscopy images which were taken from EndoCA-G2, the question came up whether only outer parts of the bigger organoids died during PAM treatment, especially with PAM concentrations of 50% and 75%.

To elucidate this matter, a live/dead Assay was performed on EndoCA-G2 and Endo-ctrl after PAM treatment (Figure 10f). Therefore, the organoids were stained with Calcein and PI, which stains living cells green and dead cells in red. Similar to the brightfield microscopy, no changes in EndoCA-G2 were seen in the control and 25% PAM concentration. A few dead cells on the margin of the organoids were detected at 50% and 75% PAM concentration whereas the internal cells of the organoids were still alive. Dead and almost completely dead organoids were seen at 100% PAM concentration. In comparison, no PAM effect was seen on Endo-ctrl.

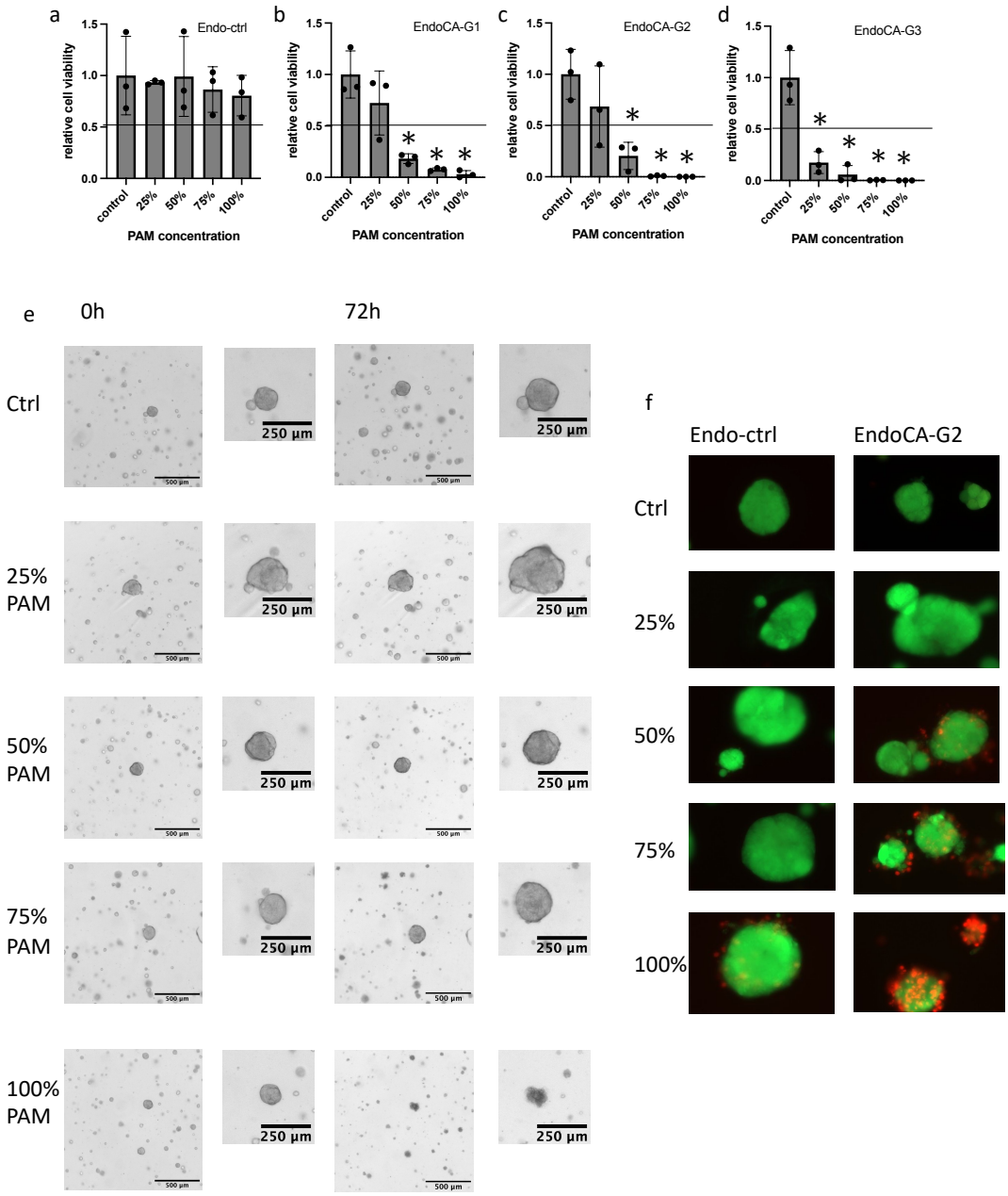

Figure 10: PAM treatment of patient-derived endometrial cancer organoids. Relative cell viability (graph) of endometrial tissue (a), EndoCA-G1 (b), EndoCA-G2 (c) and EndoCA-G3 (d) organoids. After PAM treatment with indicated PAM concentrations, 3 min PAM activation time and 24h PAM incubation time, relative cell viability was determined 72h after PAM treatment through CellTiterGlo. Representative brightfield images of EndoCA-G2 organoids (e). Images were taken before PAM treatment and 72h

after PAM treatment. Representative immunofluorescence microscopy after performing a live/dead assay on Endo-crtl and EndoCA-G2 (f). Live/dead Assay was performed 24h after PAM treatment. Data is presented as mean ± SD from n=3 independent experiments. *p < 0.05, as determined by paired t-test.

3.7. Oxidative stress in patient-derived endometrial cancer organoids rises with increasing PAM concentrations

The effect of PAM is mostly generated through reactive oxygen- and nitrogen species which have an impact on the intracellular oxidative stress level. For that reason, we investigated the oxidative stress of PAM in EndoCA-G2 organoids in comparison to healthy Endo-ctrl organoids by performing an oxidative stress assay 24 hours after PAM treatment.

The organoids were seeded out and treated with PAM like in the previous experiment with patient-derived organoids. After 24h PAM incubation time, a GSSG/GSH Assay was performed to quantify glutathione ratios of reduced glutathione (GSH) and oxidized glutathione (GSSG). High levels of GSSG are an indicator for oxidative stress, potentially leading to apoptosis or cell death.

Patient-derived endometrial cancer organoids (Figure 11a) showed an increase in GSSG/GSH ratios with increasing PAM concentrations, significantly at 50% PAM concentration (Fig. 11a; 50% PAM dilution: 5.03-fold increase, p=0.006). In comparison to endometrial cancer organoids, no significant change in GSH/GSSG ratios was seen in healthy Endo-ctrl organoids (Figure 11b).

Representative brightfield microscopy of the EndoCA-G2 organoids (Figure 11c) and Endo-ctrl organoids (Figure 11d) were taken before PAM application and before performance of the GSH/GSSG. No morphological changes were detected in Endo-ctrl and EndoCA-G2 organoids using a 50% PAM concentration. Minimal changes were observed using the 100% PAM concentration for EndoCA-G2 organoids.

This leads to the conclusion that PAM increases the oxidative stress levels in endometrial cancer organoids however not in healthy endometrial tissue.

Taken together, it solidifies the assumption that PAM exerts cancer specific effects and has no effects on healthy endometrial tissue.

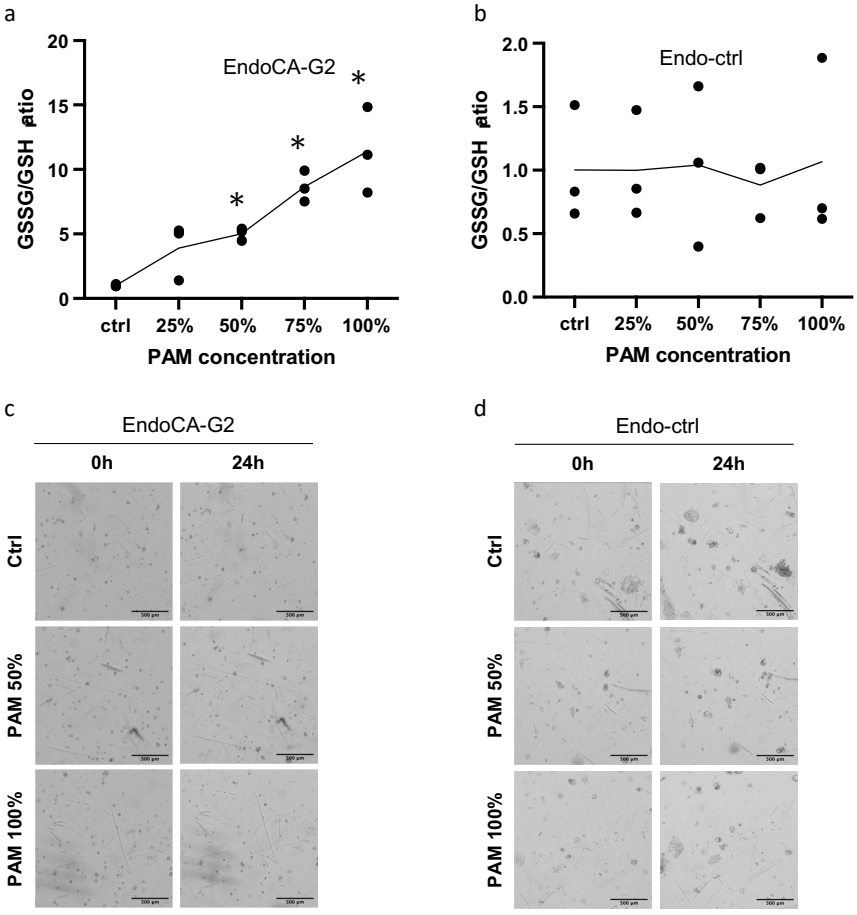

Figure 11: Evaluation of oxidative stress in endometrial cancer EndoCA-G2 organoids vs. healthy Endo-ctrl organoids after PAM treatment.

GSSG/GSH ratio (graph) and representative brightfield microscopy of the cells (insert) after 24h PAM treatment with different PAM concentrations of EndoCA-G2 (a) and Endo-ctrl (b). Data is presented as mean ± SD from n=3 independent experiments. *$p < 0.05$, as determined by paired t-test.

4 Discussion

4.1. Effects of PAM on endometrial adenocarcinoma

Plasma therapy is a promising new therapeutic option for various cancer diseases besides its primary indication for wound healing and antiseptics. PAM is already being used in the clinical routine for dermatological applications especially wound treatment. (51) However the treatment of cancer diseases with PAM has still not transitioned into the clinical routine and the clinical use of PAM as an option for cancer treatment is still subject of fundamental research. (52)

Up to this point, PAM was only tested on 2D endometrial cancer cells. This study aimed to compare PAM treatment of two-dimensional endometrial cancer cells to patient-derived three-dimensional organoids.

Nakamura et al. reported about PAM treatment of 2D ovarian cancer cells. (53) The procedure of PAM production and PAM treatment of the cells was similar to our approach. Comparing these findings of PAM effects on ovarian cancer tissue to the effects on endometrial cancer cells, numerous correspondences can be found. The PAM effects are dependent on the cell type, cell number, PAM dilution ratio as well as the exposure time. (53) Yoshikawa et al. developed PAM for clinical use and investigated the effects of PAM on endometrial cancer cell viability in vitro. Four different two-dimensional endometrial adenocarcinoma cell lines were used. Their findings showed a selective sensitivity. The cell viability after PAM treatment was reduced to varying degrees depending on the cell line. A cell type-specific sensitivity was also seen in our study: we treated two endometrial adenocarcinoma cell lines, HEC-1A and ISHIKAWA with PAM. The underlying reason for the selective sensitivity might be the different characteristics of the cell lines: although both cell lines originate from well differentiated endometrial adenocarcinoma, ISHIKAWA is a model for estrogen-dependent premenopausal EC, whereas HEC-1A was originated from a 71 years old, postmenopausal woman. Furthermore, HEC-1A and ISIKAWA show different expression profiles of the estrogen biosynthetic and metabolic enzymes. (54) Hevir-Kene et al. proposed that ISHIKAWA cells accumulate more toxic estrogen-3,4-quinones than HEC-1A. (54) Due to several expressions of different metabolic enzymes and genes in

ISHIKAWA cells, the levels of OH-estrogens and estrogen quinones are high, which results in an enormous exposure to oxidative stress. Furthermore, Williams-Brown et al. implies that in ISHIKAWA cells, estradiol acts as a tumor promoter through ERs, and as a carcinogen through the products of estrogen oxidative metabolism. (55) In contrary to ISHIKAWA, HEC-1A has a lower sensitivity for estradiol and many of the genes of phase II metabolism are more abundant in HEC-1A cells, which might lead to enhanced removal of toxic metabolites. (54) This may be a possible explanation for the higher sensitivity of ISHIKAWA cells to PAM.

Yoshikawa et al. investigated that a 0.5 h PAM incubation time with different PAM concentrations already resulted in a considerable decrease in cell viability. (52) In this study, cells were incubated with PAM for a minimum of 1h. A significant decrease in cell viability was seen after the 1 h PAM incubation time. It was seen that longer PAM treatments resulted in a significantly lower viability of cancer cells. (53, 56) In the present study, looking at cell lines in 2D cell culture, significant differences in cell viability were seen between an 1 h and 4 h treatment time. However, there was only a small difference in cell viability when comparing a 4 h and 24 h PAM treatment. Based on our results and in line with the literature we can conclude that PAM concentration as well as PAM incubation time is equally important to the reduction in cell viability. A well-balanced combination of all factors is key to a successful PAM treatment. Furthermore, Yoshikawa et al. suggested that stronger PAM should be produced for clinical use from the perspective of its anti-tumor effects. (52)

Yoshikawa et al. stated that when PAM is applied as a clinical treatment to prevent peritoneal metastasis, a shorter exposure time with PAM to the intraperitoneal cavity is necessary to minimize side effects on normal cells. (52) In this study, we treated organoids of healthy endometrial tissue with different PAM concentrations for 24 hours. No macroscopic and metabolic effects on these organoids were seen.

Nakamura et al. elucidated that oxidative stress generated through RONS plays an important role for the effects of PAM. (53) The results in their study also indicate that the anti-metastatic effect of PAM is at least partially attributed to ROS. (53) (57) Utsumi et al. investigated that PAM treatment upregulated the fraction of intracellular ROS,

which resulted in apoptosis of ovarian cancer cells. (58) Yoshikawa et al. also investigated the intracellular accumulation of ROS in endometrial cancer cells. They found that PAM induces an intracellular ROS accumulation. (52) These findings are consistent to the current hypothesis that PAM effects are due to the presence of RONS. However, these studies only investigated the oxidative stress in cancer cells and did not compare the results to healthy endometrial tissue. Previous studies have shown that PAM is selectively cytotoxic towards cancer cells. (58-60) The adverse effects of PAM on cancer cells and healthy cells was reported by many research groups: Panngom et al. showed PAM selectivity between lung cancer and embryonic fibroblasts and pulmonary epithelial cells (61), Tanaka et al. compared glioma cells and astrocytes (62) whereas ovarian cancer cells and fibroblasts were examined by Iseki et al. (63) These results align with the findings in this study in which endometrial adenocarcinoma cells were compared to healthy endometrial tissue. In our study, we investigated the oxidative stress after PAM treatment by using the GSH/ GSSG Assay which is a luminescence-based system that detects and quantifies intracellular oxidative stress by measuring reduced glutathione (GSH) and oxidized glutathione (GSSG). Normally, both forms exist in healthy cells, the majority however is reduced glutathione. A change in GSH and GSSG is an indicator for oxidative stress, potentially leading to apoptosis or cell death. We compared the oxidative stress in endometrial cancer cells to healthy endometrial tissue. We found rising levels of GSSG and falling levels of GSH in endometrial cancer cells, which is an indicator for intracellular oxidative stress. Another finding was that oxidative stress in cancer cells was upregulated and increasing with higher PAM concentrations. Cheng et al. showed that there is a correlation between the amount of RONS and the corresponding cellular effects. (64) We didn't see any changes in GSH or GSSG in healthy endometrial tissue after PAM treatment, indicating that healthy endometrial tissue can handle oxidative stress better than endometrial cancer tissue. Other studies have shown similar results concerning oxidative stress after PAM treatment of various cancer cells in comparison to healthy tissue. Therefore, it is believed that RONS, which are generated though PAM, can be used to target cancer cells without affecting the surrounding healthy tissue. (65, 66) One underlying reason for the vulnerability of cancer cells to

PAM might be that RONS can accumulate in cancer cells more easy than in healthy cells, because healthy cells generally contain more membrane cholesterol (67) and a higher number of aquaporins in their cell membranes. (66, 68) Van der Paal et al. showed that cholesterol has an influence on the penetration of certain ROS. Cancer cells have lower amount of cholesterol and therefore ingress RONS faster than their healthy counterparts. (67) They also indicate that other factors like a decreased ability to reduce redox damage in cancer cells might also play a role. (67) It is being discussed by various researchers is that tumor cells rely on different redox systems than non-tumor cells like peroxynitrite, superoxide or hydrogen peroxide. (69-71) Bauer showed that the interaction between nitrite and H_2O_2, both long-lived species in PAM, leads to peroxynitrite and singlet oxygen. The singlet oxygen causes inactivation of catalase on the surface of tumor cells. Then H_2O_2 can get into the cell though aquaporins, leading to intracellular glutathione depletion and apoptosis of the cancer cell. (69) Additionally, in contrast to non-malignant cells, malignant cells express membrane-associated NADPH oxidase (NOX1). Cancer cells need NOX1-derived superoxide anions for autocrine stimulation of proliferation. Membrane-associated catalase protects the cancer cells from NOX1-driven apoptosis-inducing signaling processes, which selectively eliminate malignant cells. (69) Therefore, it is assumed that RONS have the ability to cause the malignant cells to induce their own cell death. (69)

Another hypothesis is based on the difference in proliferation activity. (72) In healthy cells the proliferation is highly orchestrated whereas proliferation in cancer cells is constantly upregulated which leads to uncontrolled proliferation. The PAM selectivity may be explained by the presence of differences in the proliferation activity and apoptosis control systems between cancer and physiological cells. (72)

Antiproliferation is not the only effect which was found after PAM treatment. Various other cell functions like the ability to infiltrate surrounding tissue, cell migration and invasiveness as well as adhesiveness was investigated by different research groups. These findings suggested that exposure to PAM at an energy level which does not induce apoptosis reduces the metastatic invasive capacity of cancer. (72) However, the reason for the selectivity of PAM is still unexplained.

RONS are interacting with nucleic acids which results in complex DNA damage. (33, 73)
To determine DNA damage and particularly dsDNA breaks, the phosphorylation of histone H2AX at Ser139 is performed. (74) Marzi et al. showed that NIPP-induced oxidative stress leads to dsDNA breaks which is seen through rapid but transient H2AX phosphorylation. They have shown that dsDNA breaks increase significantly within 1h and 4h after NIPP treatment and decrease again 20h after NIPP treatment. (73) In the present study, we performed the H2AX stainings on 2D HEC-1A and HEC-1A organoids 12h and 24h after PAM treatment. DsDNA breaks were found in 2D HEC-1A as well as in the HEC-1A organoids. More dsDNA breaks were seen after 12h than 24h, which indicates a transient H2AX phosphorylation.
The induction of the apoptotic pathway is a well-known mechanism during NIPP treatment. (75) RONS show inhibitory impacts on metabolism and cell proliferation. (73) The resulting DNA damage was associated with downstream cell cycle arrest and the induction of apoptosis. (73, 76) DNA repair or apoptosis is initiated in case of DNA damage. Therefore, elevated expression levels of growth arrest and DNA damage-associated genes were found. (73) However, NIPP doesn't show any genotoxic or mutagenic potential. (77)
Further studies have to be performed to get more insights about the role of RONS concerning PAM treatment.

4.2. 3D endometrial cancer models in comparison to 2D cell lines

Differences must be taken into consideration when treating 2D and 3D cells with PAM. The underlying reason is that 3D cells consist of more than one cell, so they tend to have a larger volume than 2D cells and therefore need PAM in higher dosage to show effects. (78) PAM treatment time must be longer and PAM concentrations must be higher to show the same effects on 3D cells as on 2D cells.
Plasma treatment on endometrial cancer cells was so far only tested on two-dimensional cell cultures. However, conventional 2D in vitro systems have serious pitfalls which makes them not suitable for research on diseases concerning the female reproductive systems like endometrial cancer. (79)

There are still advantages of 2D cell cultures using immortalized cell lines derived from tumors concerning reproducibility and ease of access. (79) However, they lack many important features like the complexity of creating in vivo microenvironments and are therefore not representative of in vivo cell diversity. (79) Since they are mostly genetically altered, they may not represent the original tissue correctly. (80) They might even provide misleading data regarding in vivo responses. (79, 81)

3D organoids represent the in vivo situation more accurately compared to 2D cell cultures. (82) One reason for the better mimic of structural and function abilities might be the possibility of recapitulating physiological, biomechanical as well as biochemical microenvironments (82), cell-cell interactions and cell-extracellular matrix interactions. Organoids can help with a better understanding of in vivo effects.

Another relevant difference between 2D and 3D cell cultures involves their handling:

2D cell cultures grow on flat dishes with coated surfaces, typically made of plastic, where they adhere and spread. The medium consists of DMEM (with 1% P/S and 1% GlutaMax) and 10% FBS and had to be changed once or twice a week. The cells were growing quickly, and cells were harvested twice a week to perform experiments. The handling of the 2D cell cultures is usually very easy since it is well established, easy to analyze, and a lot of comparative literature is available. However, they aren't representative of real cell environments. Growing on a flat surface is not connatural to the human body, where cells are surrounded by other cells in three dimensions.

However, there are also disadvantages of 3D cell cultures like organoids. These include the complex tissue handling. (81) The cells are propagated in BME, a gel like matrix, which allows them to grow three dimensional. The medium consists of many different growth factors and other essential nutrients for the cells to ensure the growth of the organoids. The medium usually had to be changed every other day, depending on the speed of growth of the cells. The extent to which artificially induced stimulation conditions simulate the physiology of human tissues is uncertain. Organoids are each derived from only one cell clone of a cell suspension and thus may not adequately represent tissue complexity. (82)

In general, organoid technology can be seen as an alternative cell culture between in vitro and in vivo since they are providing numerous morphological, biological and pathological features of organs. (83) They have many advantages like the possibility of drug and toxicity testing, especially regarding personalized and precision medicine. (79, 84)

Endometrial cancer organoids were already successfully established by several research groups like Turco et al. (85), Girda et al. (86) and Boretto et al. (44). Turco et al. has derived organoids from endometrial adenocarcinomas from postmenopausal women. (85) These organoids represented a wide range of patient-specific morphologies and the characteristics of the organoids corresponded well to original tumor tissue. Furthermore, the reported organoids allowed the comparison of endometrial cancer tissue with healthy endometrial tissue.

A general problem, however, is the lack of stromal cells in the organoids, which are essential for mimicking physiological functions and pathological conditions. (87-89) Besides stromal cells organoids lack blood vessels, innervation, and immune cells. Recently, Stzepourginski et al. developed a culture of intestinal organoids containing stromal cells. (90) In the present study, we followed the basic principles of the previous organoid culture establishments and used the organoids for testing the sensitivity of endometrial carcinoma to PAM.

Boretto et al. (2019) successfully generated organoids from endometrial cancer samples obtained from patients diagnosed with both low-grade and high-grade tumors. Notably, these organoids accurately recapitulated the distinct cancer subtypes, faithfully preserving the molecular and cellular characteristics of their respective original tumors. (91) According to Hibaoui et al. (2020), endometrial cancer organoids present a superior model for high-throughput drug screening compared to immortalized or carcinoma-derived cell lines. Additionally, they serve as a robust tool for predicting the efficacy and safety of potential therapeutics during the preclinical stages. (82)

Although lots of research was already performed on endometrial cancer organoids, the organoid model is still in the beginning of its development and needs to be further

developed in the future. (82) Additionally, clinical studies are needed to correlate organoid assay results with patient outcomes. (79)

Treatment of endometrial carcinoma requires a deeper understanding of its individual characteristics. Therefore, in the future, advanced technologies like multi-organoid-on-a-chip and human-on-a-chip models may be able to provide a platform for the individualization of therapies and advance biomedical and preclinical pharmaceutical research. (79, 92) They would allow in-vivo-like PAM characterization and would provide a microfluid environment which is crucial for pharmacogenetic modeling and toxicology studies. (79, 92) Both techniques may significantly affect the future of medicine, especially the improvement of drug development. (79, 92, 93)

4.3. PAM in cancer therapy

There are many possible options how PAM can be effectively used in cancer therapy. However, there are also some problems which might occur. Direct plasma therapy on one hand is used for local and superficial treatment, mostly in dermatology. However, when it comes to body cavities like the abdominal cavity, the use of direct plasma is restricted. In this case, indirect plasma like PAM could be a good alternative for the treatment of non-superficial cancers. This way PAM treatment can become more feasible for a minimal-invasive application, especially for cells with are not on the surface, like endometrial cancer cells. (53) Regarding the handling of the treatment, PAM has a clear advantage over direct Plasma treatment: PAM was shown to be stable for several days under specific storage conditions. Meaning that PAM can be produced several days before the actual treatment. PAM contains long-lived RONS with lifetime ranging from hours to several days. (94) The efficiency of PAM depends on storage duration as well as storage temperature. (94)

Another important aspect which has to be taken into consideration is that around 10% of endometrial carcinoma patients fall ill during their reproductive phase. (95) A treatment is needed which is capable of maintaining fertility and preserving the ability to have children. Gotlieb at al. showed in their study that conservative treatment with progestin achieved good results, however the number of patients who achieved live

births was still not satisfying. In addition a high cancer recurrence rate was seen. (96) Therefore another therapy option must be found for these patients. PAM could be a fertility-preserving approach to cure endometrial cancer in premenopausal women since PAM is only inducing apoptosis in malignant cells and is not cytotoxic towards healthy cells. (72) In this way, healthy endometrial tissue can be preserved, which is essential for the implantation of the blastocyst.

Other positive effects of PAM treatment which can be beneficial are the inhibitory effects on motility and invasive capacity of cancer cells. A possible use of PAM could therefore be the prevention of secondary metastasis for cancer cells.

Kajiyama et al. suggests that intra-cavity treatment with PAM is thought to be one of the most effective modalities of plasma cancer therapy. (72)

However, a number of problems must be considered when it comes to in vivo application of PAM. One obstacle which might be faced in the clinical use of plasma is related to the presence of intrinsic reactive oxygen species scavengers such as glutathione which are constantly present in human body tissue. It is presumed that the PAM effects are related to oxidative stress induced by reactive oxygen and nitrogen species. Considering this, the PAM effects might decrease due to the scavengers in vivo. (72) Kajiyama et al. suggests this problem to be solved by improving the plasma irradiator and developing a method to temporarily inhibit scavengers. (72)

Furthermore, the infiltration depth of PAM on tumor surface is shallow. The inner region of the tumor cannot be penetrated by PAM if the tumor exceeds a certain size. (72) Partecke et al. reported an infiltration depth of about 50 µm from the superficial layer of the tumor. (97) In this study, we investigated the same effects and found that the infiltration depth can be increased though applying higher PAM concentrations. It is necessary to find ways on how to further improve the infiltration depth of PAM.

Another important question that needs to be faced is the choice of medium used for plasma activation. Multiple different types of media are currently tested and each one has its advantages and disadvantages. It was already discovered that CAP can form RONS in water or saline solutions such as Phosphate Buffer Saline (PBS) or Ringer's saline. Mahdikia et al. used plasma-activated water to induce apoptosis in melanoma cancer

cells in-vitro. (98) Advantages of water as the medium are the low costs, the availability and the fact that it doesn't contain any ions or macromolecules that could potentially interfere with RONS. (99) On the other hand, when plasma is activated in water, lots of H^+ ions are produced which leads to the acidification of the water and the pH decreases to 3.25. This is followed by an increased conductivity. According to Ikawa et al., a low pH is necessary to induce cell toxicity effects, however this refers to plasma which is applied on surfaces and have shown to be efficient bactericides. (100) However, acidification of the plasma might not be suitable for the application in body cavities like the uterus since the pH is close to neutral or even alkaline ranging from 7.0 - 8.0. (101) An acidic pH in the uterine cavity could affect fertility negatively. (102, 103)

Another possible medium option is Ringer's saline. One advantage of Ringer's saline is that the contained ions and macromolecules mimic those found in the human body. Therefore, it can be used to maintain physiological conditions. (99) Meteu-Sanz et al. used Plasma-treated Ringer's saline to treat osteosarcoma in vitro. They also investigated the acidification of Ringer's saline after plasma activation and found a decrease of pH to non-physiological values, ranging between 3.0 – 4.0 in a dose-dependent manner. (104) Labay et al. also showed that CAP treatment of Ringer's saline causes a progressive acidification due to the formation of nitrites. (105) Furthermore, Ringer's saline lacks nutrients to sustain cell viability. (65, 104) Therefore, Meteu-Sanz et al. added 10% FBS to the Ringer's saline after treatment which stabilized the pH between 7.1 and 7.8. (104)Tanaka et al. showed that plasma activated in Ringer's lactate led to antitumorigenic effects on cancer cells. (106) Sato et al. conducted a study in 2018 to demonstrate the antitumor effects on plasma-activated Ringer's solution in vitro and in vivo. (107)

Ringer's saline on its own might not be an applicable medium for plasma therapy in human body cavities, however, when compared with cell nutrients, it could also be a possible option. Phosphate-buffered saline (PBS) is a liquid which is quite similar to Ringer's saline. It is a buffer solution with a neutral pH which is often used in medical research. It is similar to the ions and macromolecules in the human body and it has the ability to support the survival and proliferation of cells while exposed to RONS generated

through plasma. (99) Van Boxem et al. investigated cancer cell cytotoxicity of plasma-treated PBS on different glioblastoma cancer cell lines. (108) They suggested that plasma-activated PBS is more suitable for in-vivo applications in a clinical setting than PAM due to its higher stability. They investigated the stability of RONS in plasma-treated PBS and showed stability during a 2h time period. (108)

Cell culture medium, is the medium which is mostly used for plasma activation. (99) It contains salts, proteins, glucose, amino acids as well as hormones, nutrients and growth factors which are relevant for the survival and proliferation of cancer cells. (99, 109) For the generation of RONS, it is important to consider the biochemical composition of the medium since the components of the medium can react with plasma and the RONS produced. (109) The instability of RONS in PAM are due to cysteine and methionine reacting with H_2O_2. (110) Additionally, Yan et al. found that proteins in FBS consumed RONS generated by plasma activation significantly and therefore reduced cell toxicity. (111) PAM could be stored at a temperature of -80° for 7 days. However, at room temperature the RONS decreased quickly and therefore, the cell toxicity is reduced. (112)

In this study, we decided to use Dulbecco's Modified Eagle Medium (DMEM) for the production of PAM since it is the most used medium for plasma activation and it contains a variety of different nutrients for the cells. Since the PAM treatment time for the 3D organoids was 24h, it was crucial for PAM to contain nutrients so that the endometrial cancer organoids wouldn't die due to undersupply of nutrients. PAM was freshly produced before each treatment, so storage and degradation was not an issue in our case.

Regarding cancer selectivity, PAM could be a safer cancer therapy since it is only affecting cancerous tissue and not harming the adjacent healthy cells. In contrast to this, radiotherapy as well as chemotherapy also damages healthy tissues which usually leads to several side effects during and after treatment. Adverse effects can be reduced with PAM treatment. (72) Further investigation must be performed to evaluate whether PAM is a better or equally good treatment as chemotherapeutical drugs.

Murillo er al. explored whether CAP could be used to overcome drug resistance in cancer since drug resistance in cancer treatments presents as a major problem and can even lead to a progression of the disease. (99) CAP has some advantages compared to other therapeutic options in cancer treatment. PAM doesn't show any systemic side effects since its selectivity is directed towards cancer cells. PAM can be used in versatile ways; it can be applied directly onto the tumor and therefore be effective in solid tumors. Another way of application may be intravenous administration. This leads to the ability of PAM to treat a wide range of cancer types and stages. Furthermore, CAP can be used in a combination with other drugs to enhance their efficiency. CAP could stimulate the immune system by increasing the infiltration of immune cells into the tumor, enhancing the expression of immune checkpoint molecules and stimulation the production of pro-inflammatory cytokines that promote anti-tumor immune response. These effects might also lead to an increase in effectiveness of immunotherapies. (99)

One question which needs to be further addressed in the future is how PAM can be applied in vivo, especially in body cavities. The injection of PAM in its liquid form might result in fast dilution due to other body fluids like extracellular fluids or blood. (105) One possible solution could be the application of PAM though hydrogels. Hydrogel is a very promising biomaterial based on natural polymers, synthetic polymers or a mixture between both natural and synthetic polymers. (105) Plasma treatment on hydrogel has already been tested in several studies, mostly with the target application of drug carrier or drug delivery. (113, 114) Hydrogels have proved to be a suitable biomaterial for the local delivery of drugs at physiologically relevant doses for prolonged periods of time. (105) Gorbanev et al. showed that hydrogel can be used as a carrier for RONS, which are assumed to play a major role in the mechanism of plasma therapy. (115)

Labay et al. showed that the physico-chemical structure of hydrogels was not affected by PAM treatment and even showed a larger capacity for RONS than a typical isotonic saline solution. (105) Another positive feature of hydrogels treated PAM would be the capability for a sustained RONS release. These findings allow further research on the use of hydrogel-based biomaterial for PAM therapies and open new opportunities in the

design of new implantable biomaterials for plasma therapies as a minimal invasive treatment strategy. (105)

5 Summary

Endometrial cancer is the most common tumor of the female reproductive organs in industrialized nations and a frequent disease in premenopausal women. However, fertility preserving therapeutic options remain inadequately studied.

The aim of this study was the characterization of cancer specific effects of plasma activated medium (PAM) on endometrial cancer in vitro. Firstly, PAM effects were dose-dependently tested on two endometrial adenocarcinoma cell lines, HEC-1A and ISHIKAWA. It was observed that ISHIKAWA cells are more sensitive to PAM and the cell viability was already significantly reduced at lower PAM concentrations compared to HEC-1A. These effects on ISHIKAWA and HEC-1A were also shown in a 3D organoid cell culture model using both cell lines.

Significantly reduced cell viability could also be observed in PAM treated patient-derived endometrial cancer organoids with different gradings, G1-G3. Organoids from a high-grade tumor (G3), showed a higher sensitivity to PAM compared to intermediate-grade (G2) a low-grade (G1) tumors. Healthy patient-derived endometrial organoids did not show any PAM-dependent effects on organoid proliferation.

In general, either increased PAM activation time or increased PAM incubation time was needed to deplete 3D organoid tissues.

A life/dead assay showed that PAM in lower concentrations only killed the cells on the outside of the organoids whereas high concentrations were able to kill the whole organoid due to an increased infiltration depth.

Oxidative stress in the G2 organoids compared to healthy endometrial tissue was determined after PAM treatment by measuring the GSH and GSSG levels in the cells. Oxidative stress levels in patient-derived endometrial cancer organoids were significantly rising with increasing PAM concentrations whereas no alteration was found in healthy endometrial tissue.

The application of PAM may expand the fertility-preserving therapy for endometrial carcinoma and contribute to disease control in future.

6 Zusammenfassung

Das Endometriumkarzinom ist das häufigste Malignom des weiblichen Genitaltraktes in Industrienationen und daher auch eine häufige Krebserkrankung unter prämenopausalen Frauen. Jedoch sind effiziente therapeutischen Optionen zur Erhaltung der Fruchtbarkeit nur unzureichend verfügbar.

Das Ziel der Arbeit war die Charakterisierung der krebsspezifischen Wirkungen von Plasma-aktivierten Medium (PAM) auf das Endometriumkarzinom. Zunächst wurde die Wirkung den PAM dosisabhängig an zwei Zelllinien des endometrioiden Adenokarzinoms, HEC-1A und ISHIKAWA, getestet. Es zeigte sich, dass die ISHIKAWA-Zellen empfindlicher auf PAM reagieren und die Viabilität der Zellen bereits bei niedrigeren Konzentrationen deutlich geringer war als bei HEC-1A. Diese Effekte ließen sich auch in entsprechenden Organoid-Zellkulturmodellen basierend auf beiden Zelllinien zeigen. Eine signifikante Reduktion der Zellviabilität nach PAM-Behandlung konnte auch in Patientinnen-spezifischen Endometriumkarzinom-Organoiden unterschiedlichen Tumor-Gradings (G1-G3) beobachtet werden. Organoide eines G3 Tumors, zeigten eine höhere Empfindlichkeit gegenüber PAM als Organoide eines G2 Tumors und Organoide eines G1 Tumors. Im Vergleich dazu zeigte gesundes Endometriumgewebe in der 3D Organoid-Kultur keine PAM-Effekte. Um die gleichen antiproliferativen PAM-Effekte wie in 2D Zellkultur auch in Organoiden zu induzieren, waren höhere PAM-Aktivierungszeiten oder PAM-Inkubationszeiten notwendig. Ein Life/Dead – Assay zeigte, dass durch PAM in niedrigeren Konzentrationen nur die äußeren Zellen der Organoide sterben, während bei hohen PAM-Konzentrationen das gesamte Organoid aufgrund einer erhöhten Infiltrationstiefe sterben kann. PAM-induzierter oxidativer Stress wurde im Vergleich zu gesundem Endometrium durch Messung der GSH- und GSSG-Werte in den jeweiligen Organoiden bestimmt. Der oxidative Stress stieg mit steigenden PAM-Konzentrationen in den Organoiden des Endometriumkarzinoms signifikant an, während in gesundem Endometriumgewebe keine Veränderungen des GSH/GSSG Verhältnisses festgestellt werden konnte. Die Anwendung von PAM könnte eine zukünftig eine fertilitätserhaltende Therapieoption bei Endometriumkarzinom darstellen und zur Krankheitskontrolle beitragen.

7 Literaturverzeichnis

1. Ryan AJ, Susil B, Jobling TW, Oehler MK. Endometrial cancer. Cell and Tissue Research. 2005;322(1):53-61.
2. Garg K, Soslow RA. Endometrial carcinoma in women aged 40 years and younger. Arch Pathol Lab Med. 2014;138(3):335-42.
3. Bock N, Vordermark D, Emons G. Endometriumkarzinom. Der Onkologe. 2018;24(2):177-88.
4. Morice P, Leary A, Creutzberg C, Abu-Rustum N, Darai E. Endometrial cancer. The Lancet. 2016;387(10023):1094-108.
5. Ferlay J, Soerjomataram I, Dikshit R, Eser S, Mathers C, Rebelo M, et al. Cancer incidence and mortality worldwide: sources, methods and major patterns in GLOBOCAN 2012. Int J Cancer. 2015;136(5):E359-86.
6. Southcott BM. Carcinoma of the endometrium. Drugs. 2001;61(10):1395-405.
7. Siegel RL, Miller KD, Jemal A. Cancer statistics, 2017. CA: A Cancer Journal for Clinicians. 2017;67(1):7-30.
8. Ouassou K, Klingelhöfer D, Brüggmann D. Endometriumkarzinom. Zentralblatt für Arbeitsmedizin, Arbeitsschutz und Ergonomie. 2020;70(6):287-91.
9. Suh-Burgmann E, Hung Y-Y, Armstrong MA. Complex Atypical Endometrial Hyperplasia: The Risk of Unrecognized Adenocarcinoma and Value of Preoperative Dilation and Curettage. Obstetrics & Gynecology. 2009;114(3).
10. Halla K. Emerging Treatment Options for Advanced or Recurrent Endometrial Cancer. J Adv Pract Oncol. 2022;13(1):45-59.
11. Olive KP, Tuveson DA, Ruhe ZC, Yin B, Willis NA, Bronson RT, et al. Mutant p53 Gain of Function in Two Mouse Models of Li-Fraumeni Syndrome. Cell. 2004;119(6):847-60.
12. Lax SF, Kendall B, Tashiro H, Slebos RJC, Ellenson LH. The frequency of p53, k-ras mutations, and microsatellite instability differs in uterine endometrioid and serous carcinoma. Cancer. 2000;88(4):814-24.
13. Erkanli S, Eren F, Pekin S, Bagis T. CL-2 and P53 Expression in Endometrial Carcinoma. Journal of Experimental and Clinical Cancer Research. 2004;23(1):97-104.
14. LECCE G, MEDURI G, ANCELIN M, BERGERON C, PERROT-APPLANAT M. Presence of Estrogen Receptor β in the Human Endometrium through the Cycle: Expression in Glandular, Stromal, and Vascular Cells1. The Journal of Clinical Endocrinology & Metabolism. 2001;86(3):1379-86.
15. Weihua Z, Saji S, Mäkinen S, Cheng G, Jensen EV, Warner M, et al. Estrogen receptor (ER) beta, a modulator of ERalpha in the uterus. Proc Natl Acad Sci U S A. 2000;97(11):5936-41.
16. Levine DA, Getz G, Gabriel SB, Cibulskis K, Lander E, Sivachenko A, et al. Integrated genomic characterization of endometrial carcinoma. Nature. 2013;497(7447):67-73.
17. Le Gallo M, Bell DW. The emerging genomic landscape of endometrial cancer. Clin Chem. 2014;60(1):98-110.

18. Hussein YR, Weigelt B, Levine DA, Schoolmeester JK, Dao LN, Balzer BL, et al. Clinicopathological analysis of endometrial carcinomas harboring somatic POLE exonuclease domain mutations. Mod Pathol. 2015;28(4):505-14.
19. Kuhn E, Wu RC, Guan B, Wu G, Zhang J, Wang Y, et al. Identification of molecular pathway aberrations in uterine serous carcinoma by genome-wide analyses. J Natl Cancer Inst. 2012;104(19):1503-13.
20. Concin N, Matias-Guiu X, Vergote I, Cibula D, Mirza MR, Marnitz S, et al. ESGO/ESTRO/ESP guidelines for the management of patients with endometrial carcinoma. Int J Gynecol Cancer. 2021;31(1):12-39.
21. Makker V, Green AK, Wenham RM, Mutch D, Davidson B, Miller DS. New therapies for advanced, recurrent, and metastatic endometrial cancers. Gynecol Oncol Res Pract. 2017;4:19.
22. Oaknin A, Bosse TJ, Creutzberg CL, Giornelli G, Harter P, Joly F, et al. Endometrial cancer: ESMO Clinical Practice Guideline for diagnosis, treatment and follow-up. Ann Oncol. 2022;33(9):860-77.
23. Rodolakis A, Scambia G, Planchamp F, Acien M, Di Spiezio Sardo A, Farrugia M, et al. ESGO/ESHRE/ESGE Guidelines for the fertility-sparing treatment of patients with endometrial carcinoma. Facts Views Vis Obgyn. 2023;15(1):3-23.
24. Alonso S, Castellanos T, Lapuente F, Chiva L. Hysteroscopic surgery for conservative management in endometrial cancer: a review of the literature. Ecancermedicalscience. 2015;9:505.
25. Mazzon I, Corrado G, Masciullo V, Morricone D, Ferrandina G, Scambia G. Conservative surgical management of stage IA endometrial carcinoma for fertility preservation. Fertil Steril. 2010;93(4):1286-9.
26. Kaushik NK, Ghimire B, Li Y, Adhikari M, Veerana M, Kaushik N, et al. Biological and medical applications of plasma-activated media, water and solutions. Biol Chem. 2018;400(1):39-62.
27. Ahn HJ, Kim KI, Kim G, Moon E, Yang SS, Lee J-S. Atmospheric-Pressure Plasma Jet Induces Apoptosis Involving Mitochondria via Generation of Free Radicals. PLOS ONE. 2011;6(11):e28154.
28. Arndt S, Wacker E, Li YF, Shimizu T, Thomas HM, Morfill GE, et al. Cold atmospheric plasma, a new strategy to induce senescence in melanoma cells. Exp Dermatol. 2013;22(4):284-9.
29. Bauer G, Sersenová D, Graves DB, Machala Z. Cold Atmospheric Plasma and Plasma-Activated Medium Trigger RONS-Based Tumor Cell Apoptosis. Scientific Reports. 2019;9(1):14210.
30. Fridman G, Friedman G, Gutsol A, Shekhter AB, Vasilets VN, Fridman A. Applied Plasma Medicine. Plasma Processes and Polymers. 2008;5(6):503-33.
31. Wende K, von Woedtke T, Weltmann KD, Bekeschus S. Chemistry and biochemistry of cold physical plasma derived reactive species in liquids. Biol Chem. 2018;400(1):19-38.
32. Hoffmann C, Berganza C, Zhang J. Cold Atmospheric Plasma: methods of production and application in dentistry and oncology. Med Gas Res. 2013;3(1):21.
33. Kurita H, Haruta N, Uchihashi Y, Seto T, Takashima K. Strand breaks and chemical modification of intracellular DNA induced by cold atmospheric pressure plasma irradiation. PLoS One. 2020;15(5):e0232724.

34. Winter J, Wende K, Masur K, Iseni S, Dünnbier M, Hammer MU, et al. Feed gas humidity: a vital parameter affecting a cold atmospheric-pressure plasma jet and plasma-treated human skin cells. Journal of Physics D: Applied Physics. 2013;46(29):295401.
35. Yan D, Talbot A, Nourmohammadi N, Cheng X, Canady J, Sherman J, et al. Principles of using cold atmospheric plasma stimulated media for cancer treatment. Sci Rep 5: 18339. 2015.
36. Blackert S, Haertel B, Wende K, von Woedtke T, Lindequist U. Influence of non-thermal atmospheric pressure plasma on cellular structures and processes in human keratinocytes (HaCaT). Journal of Dermatological Science. 2013;70(3):173-81.
37. Adachi T, Tanaka H, Nonomura S, Hara H, Kondo S-i, Hori M. Plasma-activated medium induces A549 cell injury via a spiral apoptotic cascade involving the mitochondrial–nuclear network. Free Radical Biology and Medicine. 2015;79:28-44.
38. Braný D, Dvorská D, Halašová E, Škovierová H. Cold Atmospheric Plasma: A Powerful Tool for Modern Medicine. International Journal of Molecular Sciences. 2020;21(8):2932.
39. Mohades S, Laroussi M, Sears J, Barekzi N, Razavi H. Evaluation of the effects of a plasma activated medium on cancer cells. Physics of Plasmas. 2015;22(12):122001.
40. Biscop E, Lin A, Boxem WV, Loenhout JV, Backer J, Deben C, et al. Influence of Cell Type and Culture Medium on Determining Cancer Selectivity of Cold Atmospheric Plasma Treatment. Cancers (Basel). 2019;11(9).
41. Schmidt A, von Woedtke T, Bekeschus S. Periodic Exposure of Keratinocytes to Cold Physical Plasma: An In Vitro Model for Redox-Related Diseases of the Skin. Oxid Med Cell Longev. 2016;2016:9816072.
42. Bernhardt T, Semmler ML, Schäfer M, Bekeschus S, Emmert S, Boeckmann L. Plasma Medicine: Applications of Cold Atmospheric Pressure Plasma in Dermatology. Oxid Med Cell Longev. 2019;2019:3873928.
43. Mannelli C, Ietta F, Avanzati AM, Skarzynski D, Paulesu L. Biological Tools to Study the Effects of Environmental Contaminants at the Feto–Maternal Interface. Dose-Response. 2015;13(4):1559325815611902.
44. Boretto M, Cox B, Noben M, Hendriks N, Fassbender A, Roose H, et al. Development of organoids from mouse and human endometrium showing endometrial epithelium physiology and long-term expandability. Development. 2017;144(10):1775-86.
45. Barker N, Huch M, Kujala P, van de Wetering M, Snippert HJ, van Es JH, et al. Lgr5^{+ve} Stem Cells Drive Self-Renewal in the Stomach and Build Long-Lived Gastric Units In Vitro. Cell Stem Cell. 2010;6(1):25-36.
46. Sato T, Vries RG, Snippert HJ, van de Wetering M, Barker N, Stange DE, et al. Single Lgr5 stem cells build crypt-villus structures in vitro without a mesenchymal niche. Nature. 2009;459(7244):262-5.
47. Karthaus Wouter R, Iaquinta Phillip J, Drost J, Gracanin A, van Boxtel R, Wongvipat J, et al. Identification of Multipotent Luminal Progenitor Cells in Human Prostate Organoid Cultures. Cell. 2014;159(1):163-75.

48. Jones PM, Drapkin R. Modeling High-Grade Serous Carcinoma: How Converging Insights into Pathogenesis and Genetics are Driving Better Experimental Platforms. Front Oncol. 2013;3:217.
49. Kopper O, de Witte CJ, Lõhmussaar K, Valle-Inclan JE, Hami N, Kester L, et al. An organoid platform for ovarian cancer captures intra- and interpatient heterogeneity. Nature Medicine. 2019;25(5):838-49.
50. Maru Y, Tanaka N, Itami M, Hippo Y. Efficient use of patient-derived organoids as a preclinical model for gynecologic tumors. Gynecologic Oncology. 2019;154(1):189-98.
51. Tiede R, Emmert S. Plasmabehandlung von Wunden. 2016. p. 73-89.
52. Yoshikawa N, Liu W, Nakamura K, Yoshida K, Ikeda Y, Tanaka H, et al. Plasma-activated medium promotes autophagic cell death along with alteration of the mTOR pathway. Scientific Reports. 2020;10(1):1614.
53. Nakamura K, Peng Y, Utsumi F, Tanaka H, Mizuno M, Toyokuni S, et al. Novel Intraperitoneal Treatment With Non-Thermal Plasma-Activated Medium Inhibits Metastatic Potential of Ovarian Cancer Cells. Scientific Reports. 2017;7(1):6085.
54. Hevir-Kene N, Rižner TL. The endometrial cancer cell lines Ishikawa and HEC-1A, and the control cell line HIEEC, differ in expression of estrogen biosynthetic and metabolic genes, and in androstenedione and estrone-sulfate metabolism. Chem Biol Interact. 2015;234:309-19.
55. Williams-Brown MY, Salih SM, Xu X, Veenstra TD, Saeed M, Theiler SK, et al. The effect of tamoxifen and raloxifene on estrogen metabolism and endometrial cancer risk. J Steroid Biochem Mol Biol. 2011;126(3-5):78-86.
56. Mokhtari H, Farahmand L, Yaserian K, Jalili N, Majidzadeh AK. The antiproliferative effects of cold atmospheric plasma-activated media on different cancer cell lines, the implication of ozone as a possible underlying mechanism. J Cell Physiol. 2019;234(5):6778-82.
57. Utsumi F, Kajiyama H, Nakamura K, Tanaka H, Mizuno M, Ishikawa K, et al. Effect of indirect nonequilibrium atmospheric pressure plasma on anti-proliferative activity against chronic chemo-resistant ovarian cancer cells in vitro and in vivo. PLoS One. 2013;8(12):e81576.
58. Utsumi F, Kajiyama H, Nakamura K, Tanaka H, Hori M, Kikkawa F. Selective cytotoxicity of indirect nonequilibrium atmospheric pressure plasma against ovarian clear-cell carcinoma. SpringerPlus. 2014;3(1):398.
59. Tanaka H, Mizuno M, Ishikawa K, Nakamura K, Kajiyama H, Kano H, et al. Plasma-Activated Medium Selectively Kills Glioblastoma Brain Tumor Cells by Down-Regulating a Survival Signaling Molecule, AKT Kinase. 2011;1(3-4):265-77.
60. Kajiyama H, Utsumi F, Nakamura K, Tanaka H, Mizuno M, Toyokuni S, et al. Possible therapeutic option of aqueous plasma for refractory ovarian cancer. Clinical Plasma Medicine. 2016;4(1):14-8.
61. Panngom K, Baik KY, Nam MK, Han JH, Rhim H, Choi EH. Preferential killing of human lung cancer cell lines with mitochondrial dysfunction by nonthermal dielectric barrier discharge plasma. Cell Death Dis. 2013;4(5):e642.
62. Tanaka H, Mizuno M, Ishikawa K, Nakamura K, Kajiyama H, Kano H, et al. Plasma-Activated Medium Selectively Kills Glioblastoma Brain Tumor Cells by

Down-Regulating a Survival Signaling Molecule, AKT Kinase. Plasma Medicine. 2011;1:265-77.
63. Tanaka H, Iseki S, Nakamura K, Hayashi M, Kondo H, Kajiyama H, et al. Selective Killing of Ovarian Cancer Cells through Induction of Apoptosis by a Nonequilibrium Atmospheric Pressure Plasma. MRS Online Proceedings Library. 2012;1469(1):9-14.
64. Cheng H, Luo J, Song K, Zhao F, Liu D, Nie L, et al. On the dose of plasma medicine: Plasma-activated medium (PAM) and its effect on cell viability. Physics of Plasmas. 2022;29(6):063506.
65. Yan D, Cui H, Zhu W, Nourmohammadi N, Milberg J, Zhang LG, et al. The Specific Vulnerabilities of Cancer Cells to the Cold Atmospheric Plasma-Stimulated Solutions. Sci Rep. 2017;7(1):4479.
66. Yan D, Talbot A, Nourmohammadi N, Sherman JH, Cheng X, Keidar M. Toward understanding the selective anticancer capacity of cold atmospheric plasma—A model based on aquaporins (Review). Biointerphases. 2015;10(4).
67. Van der Paal J, Verheyen C, Neyts EC, Bogaerts A. Hampering Effect of Cholesterol on the Permeation of Reactive Oxygen Species through Phospholipids Bilayer: Possible Explanation for Plasma Cancer Selectivity. Scientific Reports. 2017;7(1):39526.
68. Verkman AS, Hara-Chikuma M, Papadopoulos MC. Aquaporins--new players in cancer biology. J Mol Med (Berl). 2008;86(5):523-9.
69. Bauer G. The synergistic effect between hydrogen peroxide and nitrite, two long-lived molecular species from cold atmospheric plasma, triggers tumor cells to induce their own cell death. Redox Biology. 2019;26:101291.
70. Bauer G, Graves DB. Mechanisms of Selective Antitumor Action of Cold Atmospheric Plasma-Derived Reactive Oxygen and Nitrogen Species. Plasma Processes and Polymers. 2016;13(12):1157-78.
71. Bauer G. Signal Amplification by Tumor Cells: Clue to the Understanding of the Antitumor Effects of Cold Atmospheric Plasma and Plasma-Activated Medium. IEEE Transactions on Radiation and Plasma Medical Sciences. 2018;2:87-98.
72. Kajiyama H, Utsumi F, Nakamura K, Tanaka H, Toyokuni S, Hori M, et al. Future perspective of strategic non-thermal plasma therapy for cancer treatment. J Clin Biochem Nutr. 2017;60(1):33-8.
73. Marzi J, Stope MB, Henes M, Koch A, Wenzel T, Holl M, et al. Noninvasive Physical Plasma as Innovative and Tissue-Preserving Therapy for Women Positive for Cervical Intraepithelial Neoplasia. Cancers. 2022;14(8):1933.
74. Sharma A, Singh K, Almasan A. Histone H2AX phosphorylation: a marker for DNA damage. Methods Mol Biol. 2012;920:613-26.
75. Dubuc A, Monsarrat P, Virard F, Merbahi N, Sarrette JP, Laurencin-Dalicieux S, et al. Use of cold-atmospheric plasma in oncology: a concise systematic review. Ther Adv Med Oncol. 2018;10:1758835918786475.
76. Gentile M, Latonen L, Laiho M. Cell cycle arrest and apoptosis provoked by UV radiation-induced DNA damage are transcriptionally highly divergent responses. Nucleic Acids Res. 2003;31(16):4779-90.
77. Kluge S, Bekeschus S, Bender C, Benkhai H, Sckell A, Below H, et al. Investigating the Mutagenicity of a Cold Argon-Plasma Jet in an HET-MN Model. PLoS One. 2016;11(9):e0160667.

78. Merbahi N, Chauvin J, Vicendo P, Judée F. Effects of Plasma Activated Medium on Head and Neck FaDu Cancerous Cells: Comparison of 3D and 2D Response. Anti-Cancer Agents in Medicinal Chemistry. 2017;17.
79. Heidari-Khoei H, Esfandiari F, Hajari MA, Ghorbaninejad Z, Piryaei A, Baharvand H. Organoid technology in female reproductive biomedicine. Reprod Biol Endocrinol. 2020;18(1):64.
80. Truskey GA. Human Microphysiological Systems and Organoids as in Vitro Models for Toxicological Studies. Front Public Health. 2018;6:185.
81. Kapałczyńska M, Kolenda T, Przybyła W, Zajączkowska M, Teresiak A, Filas V, et al. 2D and 3D cell cultures - a comparison of different types of cancer cell cultures. Arch Med Sci. 2018;14(4):910-9.
82. Hibaoui Y, Feki A. Organoid Models of Human Endometrial Development and Disease. Frontiers in Cell and Developmental Biology. 2020;8.
83. Lancaster MA, Knoblich JA. Organogenesis in a dish: modeling development and disease using organoid technologies. Science. 2014;345(6194):1247125.
84. Kopper O, de Witte CJ, Lõhmussaar K, Valle-Inclan JE, Hami N, Kester L, et al. An organoid platform for ovarian cancer captures intra- and interpatient heterogeneity. Nat Med. 2019;25(5):838-49.
85. Turco MY, Gardner L, Hughes J, Cindrova-Davies T, Gomez MJ, Farrell L, et al. Long-term, hormone-responsive organoid cultures of human endometrium in a chemically defined medium. Nat Cell Biol. 2017;19(5):568-77.
86. Girda E, Huang EC, Leiserowitz GS, Smith LH. The Use of Endometrial Cancer Patient-Derived Organoid Culture for Drug Sensitivity Testing Is Feasible. Int J Gynecol Cancer. 2017;27(8):1701-7.
87. Senol S, Sayar I, Ceyran AB, Ibiloglu I, Akalin I, Firat U, et al. Stromal Clues in Endometrial Carcinoma: Loss of Expression of β-Catenin, Epithelial-Mesenchymal Transition Regulators, and Estrogen-Progesterone Receptor. Int J Gynecol Pathol. 2016;35(3):238-48.
88. Pineda MJ, Lu Z, Cao D, Kim JJ. Influence of Cancer-Associated Endometrial Stromal Cells on Hormone-Driven Endometrial Tumor Growth. Horm Cancer. 2015;6(4):131-41.
89. Arnold JT, Kaufman DG, Seppälä M, Lessey BA. Endometrial stromal cells regulate epithelial cell growth in vitro: a new co-culture model. Hum Reprod. 2001;16(5):836-45.
90. Stzepourginski I, Nigro G, Jacob JM, Dulauroy S, Sansonetti PJ, Eberl G, et al. CD34+ mesenchymal cells are a major component of the intestinal stem cells niche at homeostasis and after injury. Proc Natl Acad Sci U S A. 2017;114(4):E506-e13.
91. Boretto M, Maenhoudt N, Luo X, Hennes A, Boeckx B, Bui B, et al. Patient-derived organoids from endometrial disease capture clinical heterogeneity and are amenable to drug screening. Nat Cell Biol. 2019;21(8):1041-51.
92. Cui Y, Zhao H, Wu S, Li X. Human Female Reproductive System Organoids: Applications in Developmental Biology, Disease Modelling, and Drug Discovery. Stem Cell Rev Rep. 2020;16(6):1173-84.
93. Xiao S, Coppeta JR, Rogers HB, Isenberg BC, Zhu J, Olalekan SA, et al. A microfluidic culture model of the human reproductive tract and 28-day menstrual cycle. Nat Commun. 2017;8:14584.

94. Kaushik NK, Ghimire B, Li Y, Adhikari M, Veerana M, Kaushik N, et al. Biological and medical applications of plasma-activated media, water and solutions. Biological Chemistry. 2019;400(1):39-62.
95. Gotlieb WH. Fertility preserving treatments for endometrial cancer: The unanswered questions. Gynecologic Oncology. 2013;129(1):1-2.
96. Gotlieb WH, Beiner ME, Shalmon B, Korach Y, Segal Y, Zmira N, et al. Outcome of fertility-sparing treatment with progestins in young patients with endometrial cancer. Obstetrics & Gynecology. 2003;102(4):718-25.
97. Partecke LI, Evert K, Haugk J, Doering F, Normann L, Diedrich S, et al. Tissue Tolerable Plasma (TTP) induces apoptosis in pancreatic cancer cells in vitro and in vivo. BMC Cancer. 2012;12(1):473.
98. Mahdikia H, Shokri B, Majidzadeh AK. The Feasibility Study of Plasma-activated Water as a Physical Therapy to Induce Apoptosis in Melanoma Cancer Cells In-vitro. Iran J Pharm Res. 2021;20(3):337-50.
99. Murillo D, Huergo C, Gallego B, Rodríguez R, Tornín J. Exploring the Use of Cold Atmospheric Plasma to Overcome Drug Resistance in Cancer. Biomedicines. 2023;11(1).
100. Ikawa S, Kitano K, Hamaguchi S. Effects of pH on Bacterial Inactivation in Aqueous Solutions due to Low-Temperature Atmospheric Pressure Plasma Application. Plasma Processes and Polymers. 2010;7(1):33-42.
101. Lykke MR, Becher N, Haahr T, Boedtkjer E, Jensen JS, Uldbjerg N. Vaginal, Cervical and Uterine pH in Women with Normal and Abnormal Vaginal Microbiota. Pathogens. 2021;10(2).
102. Moreno I, Codoñer FM, Vilella F, Valbuena D, Martinez-Blanch JF, Jimenez-Almazán J, et al. Evidence that the endometrial microbiota has an effect on implantation success or failure. Am J Obstet Gynecol. 2016;215(6):684-703.
103. Mitchell CM, Haick A, Nkwopara E, Garcia R, Rendi M, Agnew K, et al. Colonization of the upper genital tract by vaginal bacterial species in nonpregnant women. Am J Obstet Gynecol. 2015;212(5):611.e1-9.
104. Mateu-Sanz M, Tornín J, Brulin B, Khlyustova A, Ginebra M-P, Layrolle P, et al. Cold Plasma-Treated Ringer's Saline: A Weapon to Target Osteosarcoma. Cancers. 2020;12(1):227.
105. Labay C, Hamouda I, Tampieri F, Ginebra M-P, Canal C. Production of reactive species in alginate hydrogels for cold atmospheric plasma-based therapies. Scientific Reports. 2019;9(1):16160.
106. Tanaka H, Nakamura K, Mizuno M, Ishikawa K, Takeda K, Kajiyama H, et al. Non-thermal atmospheric pressure plasma activates lactate in Ringer's solution for anti-tumor effects. Sci Rep. 2016;6:36282.
107. Sato Y, Yamada S, Takeda S, Hattori N, Nakamura K, Tanaka H, et al. Effect of Plasma-Activated Lactated Ringer's Solution on Pancreatic Cancer Cells In Vitro and In Vivo. Ann Surg Oncol. 2018;25(1):299-307.
108. Van Boxem W, Van der Paal J, Gorbanev Y, Vanuytsel S, Smits E, Dewilde S, et al. Anti-cancer capacity of plasma-treated PBS: effect of chemical composition on cancer cell cytotoxicity. Scientific Reports. 2017;7(1):16478.
109. Khlyustova A, Labay C, Machala Z, Ginebra M-P, Canal C. Important parameters in plasma jets for the production of RONS in liquids for plasma medicine: A brief review. Frontiers of Chemical Science and Engineering. 2019;13(2):238-52.

110. Yan D, Nourmohammadi N, Bian K, Murad F, Sherman JH, Keidar M. Stabilizing the cold plasma-stimulated medium by regulating medium's composition. Scientific Reports. 2016;6(1):26016.
111. Yan D. Controlling plasma stimulated media in cancer treatment application. Applied physics letters. 2014;105:224101.
112. Adachi T, Tanaka H, Nonomura S, Hara H, Kondo S, Hori M. Plasma-activated medium induces A549 cell injury via a spiral apoptotic cascade involving the mitochondrial-nuclear network. Free Radic Biol Med. 2015;79:28-44.
113. Labay C, Roldán M, Tampieri F, Stancampiano A, Bocanegra PE, Ginebra MP, et al. Enhanced Generation of Reactive Species by Cold Plasma in Gelatin Solutions for Selective Cancer Cell Death. ACS Appl Mater Interfaces. 2020;12(42):47256-69.
114. Dalei G, Das S, Das SP. Non-thermal plasma assisted surface nano-textured carboxymethyl guar gum/chitosan hydrogels for biomedical applications. RSC Adv. 2019;9(3):1705-16.
115. Gorbanev Y, O'Connell D, Chechik V. Non-Thermal Plasma in Contact with Water: The Origin of Species. Chemistry. 2016;22(10):3496-505.

8 Erklärung zum Eigenanteil

Die Arbeit wurde in der Universitätsfrauenklinik des Universitätsklinikums Tübingen unter der Betreuung von Prof. Martin Weiss durchgeführt.
Die Konzeption der Studie erfolgte in Zusammenarbeit mit Prof. Martin Weiss und Dr. André Koch.
Sämtliche Versuche wurden nach Einarbeitung durch cand. med. Juliane Scheid und Dr. André Koch) von mir eigenständig durchgeführt. Die statistische Auswertung erfolgte eigenständig.
Ich versichere, das Manuskript selbstständig verfasst zu haben und keine weiteren als die von mir angegebenen Quellen verwendet zu haben.
Teile dieser Arbeit wurden bereits publiziert in Becker,E et al., Exploring cell type-specific efficiany of plasma-activated medium (PAM) on endometrial cancer using patient-specific 2D and 3D cell culture systems. IEEE Transactions on Radiation and Plasma Medical Sciences, DOI: 10.1109/TRPMS.2024.3421601.

Tübingen, den 17. August 2024

Eva Becker